

KWAME NKRUMAH UNIVERSITY OF SCIENCE AND TECHNOLOGY

COLLEGE OF ENGINEERING

DEPARTMENT OF ELECTRICAL & ELECTRONIC ENGINEERING



Project report on:

**Power Electronic Converter Control Emulating
Synchronous Machine Characteristics**

By:

AHORSU, Etornam Komla - 9309717

CHINENYE, Chibueze Vincent - 9760813

ODEI, Kelvin Mireku - 9317217

Supervisor:

Dr. Francis Boafo Effah

September, 2021

Abstract

Renewable energy resources based distributed generation (DG) units' integration into the power system is growing rapidly, and the power system experiencing low inertia and damping, which causes severe stability and performance issues to the power system. In order to facilitate the high penetration of DGs into the existing power system, improved converter control schemes are needed to ensure power system stability. Since, the synchronous generator has underpinned the stable operation of power systems for over 100 years. It is desirable for this converter control schemes to emulate the dynamics of the synchronous generator. The idea connotes the virtual synchronous generator (VSG) concept.

In this research, a number of recent and pertinent literatures have been reviewed. The strengths and weaknesses have been stated. Improvements were made upon the weaknesses of some reviewed literatures. A study has been carried out on the synchronous generator to understand how it inherently controls grid voltage, frequency, active and reactive power. The theory underlining the control of a voltage source inverter to emulate the synchronous generator in terms of damping of oscillations, rotational inertia, active power-frequency (P-f) droop control and reactive power-voltage (Q-v) droop control is presented.

A proposed VSG control scheme of an inverter to emulate the P-f droop control, Q-v droop control and inertia property of the SG was presented. For performance evaluation, this controlled scheme together with an uncontrolled inverter is simulated in MATLAB/Simulink to investigate the effectiveness of the control system as well as identify possible areas of improvement to the control system. The simulation results are discussed and analysed. Based on the simulation results and implementation, possible areas of improvement to the control system have been made.

Table of Contents

1. INTRODUCTION	5
1.1 Background to Research	5
1.2 Aim.....	7
1.3 Objectives.....	7
1.4 Organization of Research	7
2. LITERATURE REVIEW	8
2.1 Analysis of the Synchronous Machine in its Operational Modes: Motor, Generator and Compensator by Prathamesh M. Dusane et al [5] in 2015.....	8
2.2 Adjustment of Active and Reactive Power of Synchronous Generator in Grid-connected Operation by Huiqiang Sun [6] in 2020.....	9
2.3 A comprehensive review of virtual synchronous generator by Khalid Mehmood Cheema [7] in 2020.....	10
2.4 Virtual Synchronous Generator: An Overview by O. O. Mohammed et al [8] in 2019	11
2.5 A Virtual Synchronous Machine Implementation for distributed control of power converters in Smart Grids by Salvatore D’Arco et al [9] in 2015.	12
2.6 Comparison of Virtual Synchronous Generator Strategies for Control of Distributed Energy Sources and Power System Stability Improvement by Guilherme Penha da Silva Junior et al [10] in 2020	13
2.7 Emulating Rotational Inertia of Synchronous Machines by a New Control Technique in Grid-interactive Converters by Meysam Saeedian et al [11] in 2020	14
2.8 Parallel Operation of Virtual Synchronous Machines with frequency droop control by Prabin Adhikari et al [13] in 2017.....	15
2.9 Operation Area Calculation and Parameter Analysis of Virtual Synchronous Machine by Li Junjie et al [14] in 2019.....	16
2.10 Verification of the power converter based virtual synchronous machine by Meng-Jiang Tsai et al [15] in 2016	17
3. THEORY – DESIGN CONSIDERATIONS	18
3.1 Introduction	18
3.2 The Study System – Synchronous Generator.....	20
3.3 Synchronous Generator’s Inherent Stability Mechanism.....	23
3.4 The Proposed Solution – Virtual Synchronous Generator	25
3.5 The Proposed (Specific) VSG Control Algorithm	28
4. METHODOLOGY & IMPLEMENTATION	35

4.1 Introduction.....	35
4.2 Methodology	35
4.3 Implementation	35
5. RESULTS AND DISCUSSION.....	43
5.1 Introduction.....	43
5.2 Simulation Results	43
6. CONCLUSION AND FUTURE WORK	53
6.1 Conclusion	53
6.2 Future Work	53
7. REFERENCES	55

Acknowledgements

Firstly, we thank the Almighty God for the physical strength and mental fortitude He granted us for the successful completion of the project.

We would like to express our profound gratitude to Dr. Francis Boafo Effah, our project supervisor, for his guidance, encouragement and useful critiques to the completion of the project.

We would also like to extend appreciation to all the lecturers and technicians at the Department of Electrical and Electronic Engineering, KNUST for their immense contribution in various ways to help bring fruition to the project work.

1. INTRODUCTION

1.1 Background to Research

Power systems are arguably the most important infrastructure that underpins social life and economic growth. It is regarded as the largest and most complex machine engineered by humankind (Kundur 1994). The existing power generation system is dominated by large centralized power plants such as large thermal and hydro plants. However, these facilities pose two major challenges;

1. Technological and Economic: These plants usually have a fixed installed capacity to meet an ever-increasing demand for electricity and an increase in installed capacity would come at a very huge cost. Also, the transmission of electricity from such plants to distant locations, for example, rural areas, would be expensive since substations and long transmission lines with adequate insulation would be employed.
2. Environmental: Large thermal plants that burn fossil fuels such as coal, oil and gas emit greenhouse gases, for example, carbon dioxide (CO₂) which is a major cause of climate change. In 2014, the European Union's (EU's) 280 coal plants released 755 million tonnes of CO₂ – representing around 18% of the EU's total greenhouse gases [1].

The large scale adoption of renewable energy (RE) based distributed generations (DGs) has been widely adopted as a promising means of tackling these two challenges. The share of renewable energy in the power sector would increase from 25% in 2017 to 85% by 2050, mostly through growth in solar and wind power generation [2].

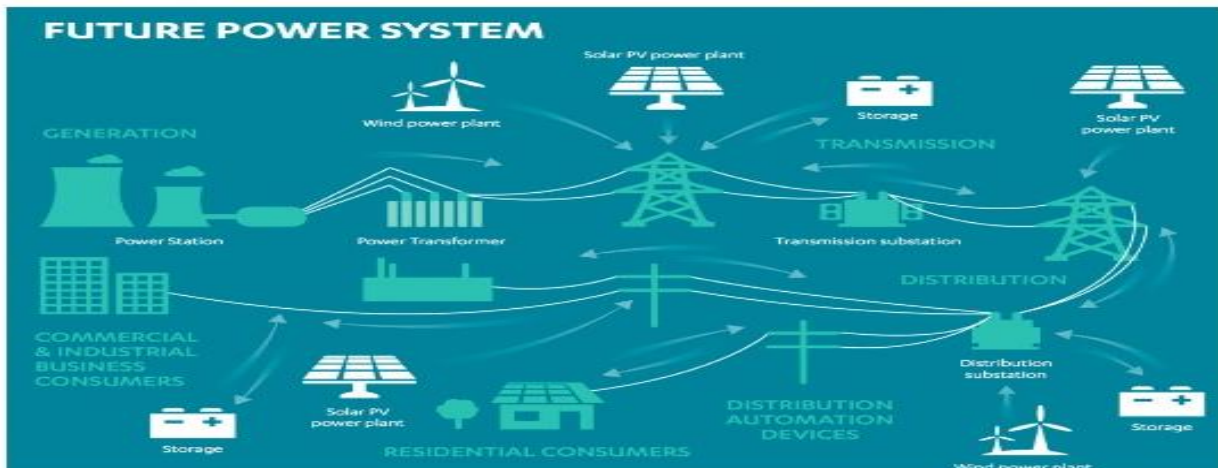


Figure 1.1 The future power system (combination of centralized and decentralized power facilities)

The non-white part shows the traditional or conventional power system and the white together with the non-white part is the future power system. This reflects the idea that decentralized and bulk power systems are complementary, nevertheless some coal power plants have been decommissioned due to the high amount of greenhouse gas they emit.

Main Problem or Challenge

Conventional centralized power systems, where power is generated mostly by large synchronous generators (SGs), with speed governor and excitation control, can support power system stability due to inherent rotor inertia by means of a large rotating part, damping characteristic, and voltage (reactive power) control ability. **However, most DGs such as photovoltaic and wind systems need power electronic interface circuits to connect to the grid, but these devices can not inherently provide enough inertia and damping characteristics, due to the lack of a rotating part.** Thus, the inverters lack the flexible voltage regulation and frequency modulation capability of SGs.

Consequently, a high penetration of these inverters would make the power system vulnerable to disturbances and system faults.

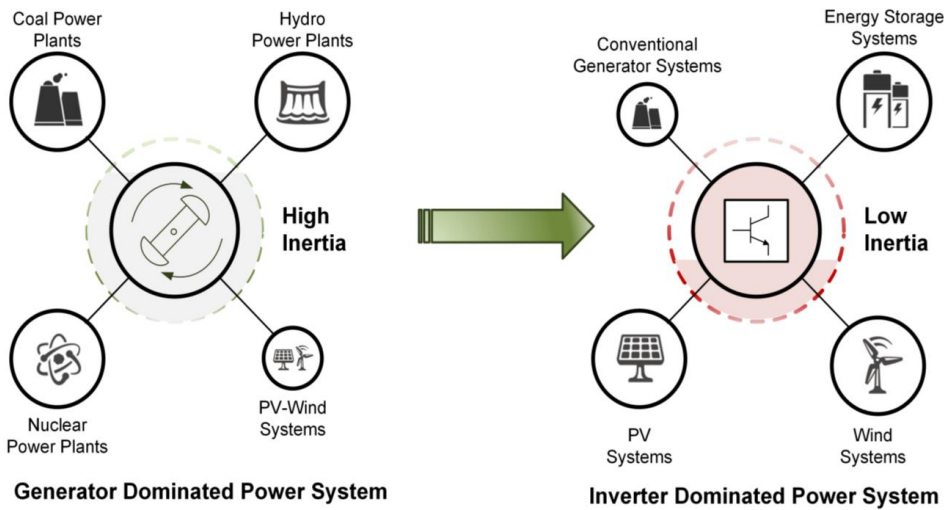


Figure 2. Low inertia in the future power system due to increased inverter-based distributed generation [3]

Effect of Problem: Power systems with lower inertia, experience a **lower minimum frequency** alongside a **high rate-of-change-of-frequency (ROCOF)** in a frequency event (generation-demand imbalance) [3]. Such situations can lead to **tripping of under-frequency relays resulting in power outages**. The European Network of Transmission System Operators for Electricity (ENTSO-E) have reported increased frequency violations in the Nordic grid correlated with increased RES penetration [4].

Therefore, there is an urgent need for a technology to enable these new energies participate in the power and frequency regulation of the power grid to support the high penetration of RES.

1.2 Aim

The aim of this research is to design and investigate power electronic control technique(s) that emulate synchronous machine characteristics in terms of providing power system stability.

1.3 Objectives

The objectives for this project are:

1. Review recent literature on synchronous machines for the control of essential parameters of power systems such as grid frequency and grid voltage.
2. Identify how power converters can be made to emulate synchronous machines in terms of rotational inertia, damping of oscillations, active and reactive power control.
3. Use MATLAB/Simulink to demonstrate the emulation of active power versus frequency (P-f) droop control and reactive power versus voltage (Q-v) droop control of power electronic converters.

1.4 Organization of Research

The research is presented in six chapters:

- Chapter 1: Introduction. This chapter presents the background to research, the motivation, the aims and objectives of the research.
- Chapter 2: Literature Review. This chapter reviews related works in the literature.
- Chapter 3: Theory – Design Considerations. This chapter presents the concepts used in the design of the proposed inverter control system.
- Chapter 4: Methodology and Implementation: The methods employed in getting the project done are presented in this chapter.
- Chapter 5: Results and Discussion. Results on the proposed control scheme are presented and analysed.
- Chapter 6: Conclusion and Future work. This chapter summaries the key achievements of this research and possible areas of development.

2. LITERATURE REVIEW

A significant number of literatures on synchronous machines (SMs) and power electronic converter (PEC) strategies that emulate (SMs) have been reviewed. The purpose for the reviews is to enable us keep pace with recent works on PEC control strategies to emulate SMs and also to serve as a guide for our project.

2.1 Analysis of the Synchronous Machine in its Operational Modes: Motor, Generator and Compensator by Prathamesh M. Dusane et al [5] in 2015

This paper describes the construction, operating principles and applications in the different operational modes of synchronous machines. The paper emphasizes the advantages of the synchronous machine as a compensator in power system networks. The machine construction is classified based on the shape of its rotor; salient pole and cylindrical rotor. The rotor with permanent magnets or electromagnets rotates in synchronism with the rotating magnetic field (RMF) created by the stator. Generator action is when the rotor runs faster than the synchronous speed of the machine and motoring action occurs when the rotor is dragged behind the air-gap flux by retarding torque of a shaft-load. A synchronous compensator is a synchronous motor whose shaft is allowed to rotate without any load. The relationship between the rotor speed, the number of poles and frequency of synchronous machines is given by

$$N_s = \frac{120f}{P} \quad (2.1)$$

The synchronous generator must run in over-excited mode to supply active power to resistive loads and reactive power to inductive loads. But when run with under-excitation, it absorbs reactive power system from the system. Inertia is an inherent feature of the synchronous compensator, and enables the machine to provide limited voltage support during very short power drops. The paper uses phasor diagrams in analysing the various operating modes.

Strengths

1. The paper highlights some features of the synchronous machine which enables it to regulate power flow of electrical transmission systems.
2. The paper reviews the conditions under which a synchronous machine can be made to generate or absorb reactive power to aid in grid voltage regulation.

Weaknesses

The paper does not discuss the inherent properties of a synchronous generator that are critical in stable and reliable operation of a power system such as;

1. Inertia due to rotating masses
2. Damping characteristic of the damping windings in the rotor
3. Speed-droop characteristics for load sharing

2.2 Adjustment of Active and Reactive Power of Synchronous Generator in Grid-connected Operation by Huiqiang Sun [6] in 2020

This paper analyses the internal process of active and reactive power regulation of a synchronous generator connected in parallel to an infinite grid, grid voltage (V) and grid frequency (f) are assumed constant, during adjustment. The internal process was analysed using phasor diagrams and power angle (δ) characteristics. To analyse the active power regulation of the generator, the input power to the prime mover is adjusted while keeping the field current constant and vice versa to analyse the reactive power regulation. The δ increases as the electromagnetic torque developed in the generator (P_m) increases. Consequently, an increase in the active power of the generator causes a decrease in reactive power, provided that excitation current and grid voltage are constant. But the change in reactive power can be corrected by adjusting excitation. When excitation current is reduced under normal excitation, the generator absorbs inductive reactive power from the grid in addition to sending active power to the grid.

$$P_2 \approx P_m = \frac{mUE_0}{X_s} \sin\delta \quad (2.2)$$

$$P_2 = mUI \cos\varphi \quad (2.3)$$

m – number of phases, U – grid voltage, I – armature current, P_m – power developed by the SG, P_2 – active power output, X_s – synchronous reactance

Advantages/Strengths

1. The paper demonstrates the power angle characteristics of active and reactive power regulation of synchronous generators.
2. The paper explains regulation methods of active and reactive power of synchronous generators.

3. The paper specifies the power angle which should not be exceeded in the power regulation of synchronous generators.

Disadvantages/Weaknesses

1. The paper fails to mention an automatic means of adjusting active and reactive power of synchronous machines in response to changes in grid parameters such as voltage and frequency.
2. The paper fails to discuss the active power-frequency and reactive power-voltage droop characteristics of synchronous generators.

2.3 A comprehensive review of virtual synchronous generator by Khalid Mehmood Cheema [7] in 2020.

This paper presents a detailed review of the basic and improved ideas of different Virtual Synchronous Generator (VSG) control techniques, modifications in VSG control and VSG implementation. The paper defines VSG as a combination of control algorithms, renewable energy sources, energy storage systems, power electronics that emulates the inertia of a conventional power system. The virtual inertia topologies analysed by the paper are Synchronverters, Topology developed in ISE lab, KHI topology, VISMA and IEPE topologies. The ISE lab topology is based on the swing equation while all others analysed in the paper are based on the full mathematical model of an SG. The swing equation of SG is used as a core part of VSG as it captures the inertia and damping properties of an SG. VSG classification based on model's order was presented. The mathematical equations for active and reactive power loop of VSG was given. The two broad categories of the control algorithm of VSG, active and reactive power control and frequency and voltage control, were analysed. While the former is used widely in grid-connected operation, the latter is used widely in islanded VSG units. VSG stability analysis were carried out using Matlab/Simulink and VSG applications were presented.

Advantages/Strengths

1. The paper highlights the key features of the different virtual inertia implementations. This provides insight for the selection of a study topology in designing our VSG.
2. The paper shows how synchronous generator (SG) modelled equations are employed in VSG operation.

3. The paper gives a detailed analysis of two broad categories of VSG control. This provides insight for the selection of a control method in designing of our VSG.

Disadvantages/Weaknesses

1. The paper fails to show how the parameters used in the control of a VSG can be estimated.
2. The paper fails to discuss the operation of multiple VSG in parallel in grid connected mode.
3. The paper discusses explain for how power would be shared between an SG and a VSG in grid connected operation.

2.4 Virtual Synchronous Generator: An Overview by O. O. Mohammed et al [8] in 2019

This paper presents an overview of VSG control mechanisms, it provides the concept, features and the review of the existing models as well as highlighting the necessary improvement that needed to be done for proper control of DGs. This paper discusses three essential inherent properties of synchronous machines that are important for a stable and reliable operation of a power system, namely: the inertia due to rotating masses, damping effect due to damper windings and the speed-droop characteristics for load sharing. The inertia and damping characteristics of a VSG can be captured by the general swing equation. The VSG has three distinct components namely: PEC (power electronic converter), an energy storage device and the control scheme that controls the power exchange between energy storage system (ESS) and power system. The ESS allows the VSG to absorb or inject power into the system. Any VSG application involves a direct mathematical model of a SG. The power output equation of a VSG was presented. The first VSM based control technique modelled the two windings of the static in the d-q frames and the inertia without any current loops. But subsequently, current control loops and virtual impedance have been added to improve the performance of the VSG. The paper uses block diagrams to demonstrate some VSG control schemes.

Advantages/Strengths

1. This paper presents the swing equation of SGs which is used in the inertia and damping emulation of SGs in PEC control.

2. The paper modifies an existing VSG model which provides more insight to the concept of VSG design.

Disadvantages/Weaknesses

1. The paper fails to provide simulations or laboratory tests of the modified VSG control techniques to give credibility to their submissions.
2. The paper fails to show how the parameters in the presented VSG control techniques can be estimated.

2.5 A Virtual Synchronous Machine Implementation for distributed control of power converters in Smart Grids by Salvatore D'Arco et al [9] in 2015.

This paper presents a specific VSM implementation in detail together with its mathematical model. The VSM implemented was based on the emulated swing equation of SGs and provided references for cascaded voltage and current controllers by measuring grid active and reactive power. The modelling, analysis and control of the electrical system of the VSG was implemented in Synchronous Reference Frames (SRFs). The mathematical model and functional block diagram was given for some subsystems of the VSM. These subsystems include Reactive Power Control, Virtual Inertia and Power Control, Virtual Impedance, Voltage Control, Current Control and Active Damping. The virtual impedance emulates the quasi-stationary characteristics of the synchronous impedance in a traditional SM. Matlab/Simulink was used to access the dynamic response of the VSM implementation to change in loading. The VSM model presented was used to establish a linearized small-signal state-space representation. Lastly, root locus plots were used to ascertain the stable range of the system parameters.

Advantages/Strengths

1. The mathematical model of all system elements are presented and this serves as a basis for design.
2. The stability tests carried out provides insight for the design and analysis of our proposed VSG algorithm.

Disadvantages/Weaknesses

1. The switching effects of the Voltage Source Converter (VSC) such as switching losses and high frequency noise were neglected.

2. The paper presents only simulation results but not experimental results.

2.6 Comparison of Virtual Synchronous Generator Strategies for Control of Distributed Energy Sources and Power System Stability Improvement by Guilherme Penha da Silva Junior et al [10] in 2020

This paper presents a literature review and performance tests for the main VSG topologies used in DGs/RESs: ISE, VSYNC, VISMA and Synchronverter. It was observed that the Synchronverter possess advantages over the other VSG topologies, capable of larger injections of active power in to the grid and capacity of automatic regulation of active and reactive power via frequency and voltage droop control. The control structure for the mentioned VSG topologies was presented. The choice of the topology used depends on the desired level of similarity to the dynamics of SG.

Table 1 Comparison of various VSG topologies presented in the paper

VSG Topology	Key Features	Weaknesses
VSYNC	Simple implementation Frequency-power response based	Instability due to PLL, particularly in weak grids.
ISE	Swing equation based Simpler model compared to SG model	Power and frequency oscillations
VISMA	Accurate replication of SG dynamics through detailed mathematical model	High number of parameters to be adjusted and uncontrollability of voltage amplitude and frequency.
Synchronverter	Full mathematical model of SGs	When PLL is used, it adversely affects synchronization of VSI

The topologies were simulated with a sampling frequency of 100 kHz and the switching frequency of the VSI was 10 kHz. All VSG topologies were tested under the same grid parameters.

Strengths

1. The simulations demonstrate the ($P-\omega$) and ($Q-V$) droop control ability of the main VSG topologies.

2. Simulation results confirmed earlier literature reports.
3. All parameters used in the simulation were presented, hence the simulation can easily be replicated.

Weaknesses

1. The switching effects of the voltage source inverter (VSI) for each VSG topology was not presented.
2. The paper fails to show how the simulation parameters were selected and hence failed to specify their stable range.

2.7 Emulating Rotational Inertia of Synchronous Machines by a New Control Technique in Grid-interactive Converters by Meysam Saeedian et al [11] in 2020

The contribution of this paper is a new control scheme for grid-tied voltage source converters. The proposed control scheme is composed of a conventional inner current loop, outer voltage loop, and a new synthetic inertia function. The virtual inertia loop provides primary frequency support through discharging or charging a DC link capacitors of VSCs employed in power electronics-based generators, for example, solar and wind farms. The paper by means of a control block diagram demonstrates the frequency response control of a SG. The synchronous reference frame transformation introduced by the PLL dynamics is also included in the control system for the required compensation. The dynamics model of the proposed scheme is built and the bode-plot and zero-pole analyses confirms that the proposed controller can perform in a stable operating condition. The stability analyses depicted that the proposed controller has a **better performance** compared to [12] in terms of the system stability margin. Simulations were conducted in MATLAB to demonstrate the validity of the proposed technique. The simulations illustrated that the rate of change of frequency **is improved** by 47.37% and 23.1% compared to the conventional controller and the method in [12], respectively.

Strengths

1. The DC-link capacitance applied as the energy buffer for grid inertia augmentation does not impose any extra cost on the VSC hardware. This is because the DC-link capacitors are essential for voltage support and harmonics filtering in power conversion systems.
2. The new control scheme gives better system stability margin and inertial response of the converter as compared to method in [12].

Weaknesses

1. The paper fails to discuss in detail the effects of switching (high frequency noise and losses) of the VSC in the proposed control scheme.
2. The paper fails to discuss how the electrical values of the components of the proposed scheme can be estimated in specific application scenarios.

2.8 Parallel Operation of Virtual Synchronous Machines with frequency droop control by Prabin Adhikari et al [13] in 2017

This paper presents a control logic for parallel operated VSMs to share transient load in proportion to their respective capacities. This concept is of great importance in an interconnected power system with multiple PV-Hydro micro-grids, where a number of VSMs need to be operated in parallel. The control logic is implemented through a frequency droop based controller.

$$P_{VSM} = K_I \frac{d\Delta f}{dt} + K_p \Delta f \quad ()$$

P_{VSM} - Power output of VSM, K_p – emulated damping constant, K_I – emulated inertia constant, f – system frequency

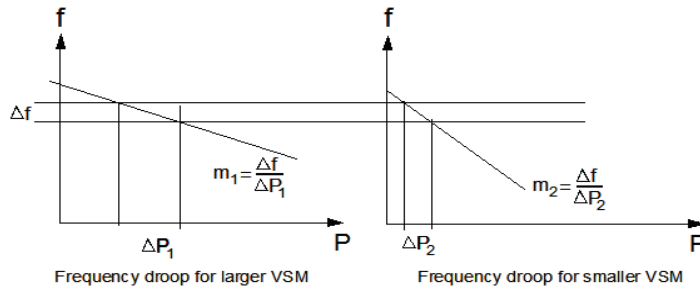


Figure 3. Frequency droop setting for parallel operation of multiple VSMs

The frequency droop based controller is achieved by selecting suitable values for K_I and K_p for each VSM to enable the two VSMs share transient loads according to their respective capacities. The damping constant K_p is equal to the slope m . The slope m_1 of the larger VSM is less than the slope m_2 of the smaller VSM, hence for the same change in system frequency the larger VSM would pick up more load as compared to the smaller VSM. The control logic is simulated in MATLAB/Simulink. The maximum allowable frequency deviation and ROCOF ($\pm 2\%$ and $\pm 1\%$ respectively) during normal steady state operation were used to set the values for K_I and K_p in each VSM. The simulation results verify that the transient power was shared between the VSMs in proportion to their capacities.

Strengths

1. This paper gives a Simulink representation of a control logic to operate VSMs in parallel and that of a detailed VSM block as well.
2. This paper shows how the design parameters (K_I and K_p) of the VSM can be estimated.

Weaknesses

1. The effect of the impedance of the line in a network of micro-grids, when multiple VSMs are installed in different locations of a micro-grid, on proportional load sharing was neglected.
2. The effect of line impedance on the performance of PLLs was neglected.

2.9 Operation Area Calculation and Parameter Analysis of Virtual Synchronous Machine by Li Junjie et al [14] in 2019

In this paper, a complete scheme is proposed for the design of the parameters of the virtual synchronous generator. The parameters required for synchronous inverter control are; active loop damping coefficient D_p , reactive loop droop coefficient D_q , active loop inertia coefficient J , and reactive loop equivalent coefficient K . By establishing the transfer function of the active and reactive loops, the four parameters are applied. The selection range of the parameters is restrained for the active power loop from the stability, the stability margin and the overshoot. For reactive power loop, the range of parameter selection is restrained from the stability and the cut-off frequency of low-pass filter. The zero-pole distribution map, the Bode plot and the step response curve are used to comprehensively analyse the influence of the VSG parameters over the steady state and dynamic performance of the system. The operating boundary of the VSM is determined, and the system parameters are adjusted according to the system performance. The simulation of the parameters is carried out in PSCAD/EMTDC to prove the feasibility of the method proposed in this paper. The selection range of parameters can be narrowed further to meet the standards of the power grid.

Strengths

1. This paper provides a blueprint for the estimation of VSG design parameters.

2. The conclusions in the paper can be applied to adjust VSG design parameters in theoretical or practical engineering.

Weaknesses

1. The paper fails to show filter parameters can be estimated in order to minimize the frequency noise due to switching of the inverter's power transistors.
2. The paper presents only simulation results but not experimental results.

2.10 Verification of the power converter based virtual synchronous machine by Meng-Jiang Tsai et al [15] in 2016

This paper investigates the effectiveness of VSM based on three-phase voltage converter. The VSM-based control algorithm investigated is based on a simplified model of the SM. The paper investigates the VSM-based power sharing control for single and parallel connected DICs (Distributed Energy Resources (DERs) interface converters), and compares the performance with the conventional droop control. The analysis indicates that the VSM-based control with a virtual inertia can be equivalent to the conventional droop control with a first order (Low Pass Filter) LPF while the frequency variation is small, and hence the VSM-based control can effectively slow down the dynamic behaviour during transient. Nevertheless, both controls have a weak point, thus, the MG (micro grid) frequency may be deviated from the nominal value at steady state. Hence, a frequency restoration mechanism is presented to regulate their frequency within the permissible ranges. Lastly, laboratory test results are provided to validate the effectiveness of VSM-based control.

Strengths

1. The paper investigates the VSM-based power sharing control for parallel connected DICs. This provides insight for multiple VSG operation.
2. The paper demonstrates how VSG-based control can be compared to conventional droop control in terms of power sharing.
3. Laboratory or experimental tests were carried out to confirm the effectiveness of VSM-based control.

Weaknesses

1. The paper fails to show how experimental set up or simulation parameters were estimated.
2. The switching effects of the inverter in the VSM-based control was neglected.

3. THEORY – DESIGN CONSIDERATIONS

3.1 Introduction

This chapter presents a study of the conventional synchronous machine. The aim of this study was to emulate the rotational inertia, damping of oscillation, active-power frequency droop characteristics (P-f) and reactive-power droop characteristics (Q-v) in the control of a three-phase voltage source inverter (VSI). This idea of operating an inverter to mimic a synchronous generator connotes the VSG concept. The VSG concept is explained and implemented in this chapter.

General Concept of Power System Control

When there is a **generation-demand imbalance** (of active and/or reactive power), **generators** and **inverters** work together to ensure synchronization, voltage stability, power balance, load sharing and economic operation [16]. Synchronization is the process of matching the frequency of a generator or other source (sub-network) to that of a running network. Two segments of a grid cannot exchange AC power unless they are in synchronization [17]. The total power, also called the apparent power S , is defined by:

$S = P + jQ$. The active power, transmitted across a purely inductive line between point 1 and point 2 has a relation with the frequency:

$$2\pi \int f = \frac{PX}{|U_1||U_2|}$$

where X is reactance f is system frequency, $|U_1|, |U_2|$ are the voltage magnitude at point 1 and point 2 respectively. Likewise, the reactive power has a relation with difference in voltage magnitude:

$$|U_2| - |U_1| = \frac{QX}{|U_2|}$$

This means that in order to control P and Q one can control the system frequency and the difference in voltage magnitude. Basically, a synchronous generator uses the swing equation to control frequency and the inverter is using droop control to regulate the frequency and voltage magnitude. The active power droop equation relates a change in active power with respect to the nominal active power, P_0 , to a change in frequency with respect to the nominal frequency f_0 . The relation is controlled by the active droop coefficient, k_p . This yields the following active droop equation:

$$f = f_0 - k_p (P - P_0) \quad (3.1)$$

Likewise, the reactive power droop equation relates a change in reactive power with respect to the nominal reactive power, Q_0 , to a change in voltage magnitude with respect to the nominal voltage magnitude E_0 . The relation is controlled by the reactive droop coefficient, k_q . This yields the following reactive droop equation:

$$E = E_0 - k_q (Q - Q_0) \quad (3.2)$$

Parallel Operation or Load sharing

When a load or demand increases, multiple parallel units with their individual droop characteristic can react to the fall in frequency by increasing their active power outputs simultaneously. The increase in active power will counteract the reduction in frequency and the units will settle at active power outputs and frequency at a steady-state point on the droop control characteristic. The same thing holds for the voltage droop control [16].

There are some levels of hierarchy in the control of generators and inverters [16].

Primary control

This level is concerned with rapidly balancing generation and demand and sharing load among multiple generating units. It also includes synchronizing the AC voltage frequencies and stabilizing their magnitudes. The primary control is accomplished by decentralized (individual units) droop control, where generating units are controlled such that their output frequency and voltage magnitudes are proportional to changes in the demand. This type of control is the focus of the project, with emphasis on the droop control.

Secondary control

This level seeks to correct steady state errors in frequency and voltage magnitudes induced by the droop controllers (used in primary control). The correction is achieved by a secondary control layer and would require power transfer with an external source. This type of control is explained briefly.

Tertiary control

This level deals with load sharing among the units, or dispatch of generation plants to minimize optimal costs. However, this type of control is not the focus of the project.

3.2 The Study System – Synchronous Generator

There are different power plants, such as coal-fired, nuclear, and hydro plants, in existing power systems. However, electricity generation is dominated by only one type of electric machine – synchronous machines. Synchronous generators are a type of synchronous machines that convert mechanical power to AC electric power. Most of the world's power system are three-phase system and hence synchronous generators are three phase machines.

The constructional features of the SG are stator, rotor, damper windings, slip-rings or collector rings, brushes and bearings. The stator unit is the stationary part of the machine and consists of the stator frame or yoke and the armature coils through which AC flows through. The rotor, which is the rotating part of the machine, which is cylindrical or drum-shaped. The core is built of steel laminations with slots to house the field windings through which DC current flows. In addition to the DC winding the rotor also carries the damper winding which produces forces which dampen the oscillation of the rotor, thereby reducing hunting (momentary speed fluctuations). The slip-rings facilitate the collection of current from the DC excitation source to the field windings. The brush and bearings carry current from the external circuit to the commutator.

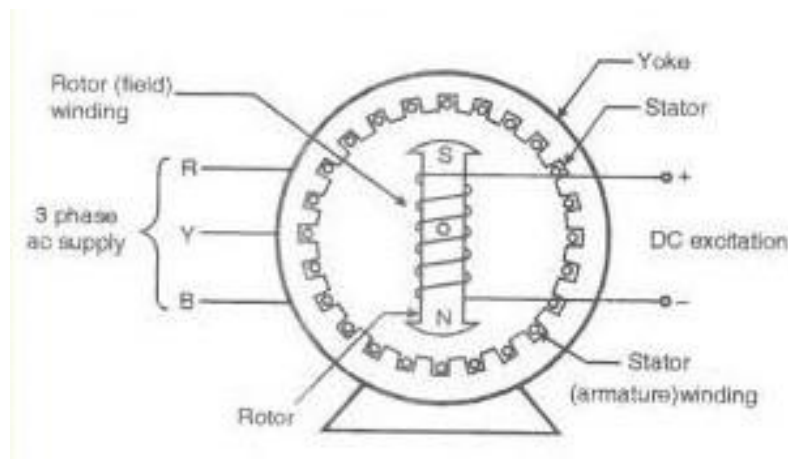


Figure 3.2.1 Synchronous generator construction [18]

The rotor is made to rotate by the turbine of a prime mover, the stator or armature conductors (being stationary) are cut by the rotated DC magnetic flux from the field coils on the rotor. Most of these plants use fossil fuel (coal, gas, oil) as primary sources of energy to drive the prime mover. According to the Faraday's principle of electromagnetic induction, emf is induced in the armature conductors. This is because the magnetic poles are alternate N and S, they induce an emf and hence current in the armature

conductors, which first flow one direction and then in the other. Hence, an alternating emf is induced in the stator windings whose frequency depends on the number of N and S poles moving past a conductor in one second and whose direction is given by Fleming's Right-Hand Rule. The voltage generated in each of the three phases would have the same magnitude, same frequency but would have a 120° phase shift from each other, since the coils within the stator are displaced in this manner.

Primary Control of a Synchronous Generator (SG)

In conventional power plants, when there is an imbalance between load demand and electric power supply, then this difference will either enter into or exist from kinetic storage. As the kinetic energy depends on the generator speed, an active power imbalance will translate into a speed (and hence frequency) deviation. Thus, if there is a momentary surplus of generator power over load, the total generator speed will increase. Conversely, when load increases and there is a momentary deficit of generator power, the generator speed would decrease. As mentioned in section 3.1, the change in active power will counteract the change in frequency and the unit will settle at active power output and frequency (at a steady-state point) on the droop control characteristic. The rate of the speed (or frequency) would depend on the amount of power imbalance and **the total moment of inertia of the running equipment**. These two parameters are thus factored in determining a regulation constant or droop constant for the synchronous generator. The magnitude of the output voltage of the generator also varies inversely proportional to reactive power demand.

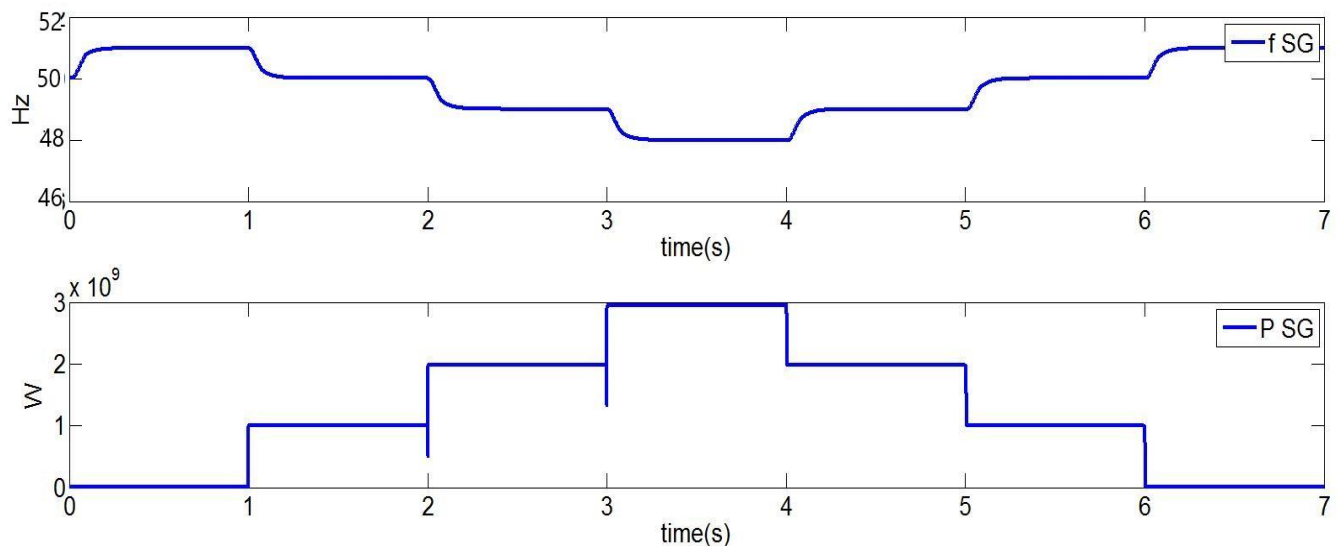


Figure 3.2.2 Primary control of an SG (system frequency and active power vary inversely according to P-f droop characteristic) [16]

In figure 5, the active power output of the SG varies inversely proportional to the system frequency according to the P-f droop characteristic. Initially, the system frequency was approximately 50 Hz but decreased with an increase in active load and vice versa.

Secondary control of a Synchronous Generator (SG)

To achieve secondary control of the SG, a closed automatic load frequency control loop (ALFC) and a closed automatic excitation control loop (AEC). Automatic load frequency control loop (ALFC) controls the generator output hence, frequency via speed governor and control valves [19]. In the event of power imbalance, the ALFC senses the system frequency, compares it to a reference frequency and adjusts the mechanical input to the prime mover (steam, hydro or gas turbines). This is to ensure active power balance and maintain system frequency at its reference value. The secondary control loop of (ALFC) maintains a fine adjustment of frequency and active power based on active power-frequency (P-f) droop characteristics. An automatic voltage regulator (AVR) regulates the terminal voltage, hence reactive power via controlling the generator excitation [19]. The AEC senses the system voltage, compares it to a reference voltage and adjusts the rotor excitation accordingly. This is to ensure reactive power balance and maintain grid voltage at its reference value. Also, the two control schemes are essentially non-interacting, that is the control of one does not significantly affect the other one.

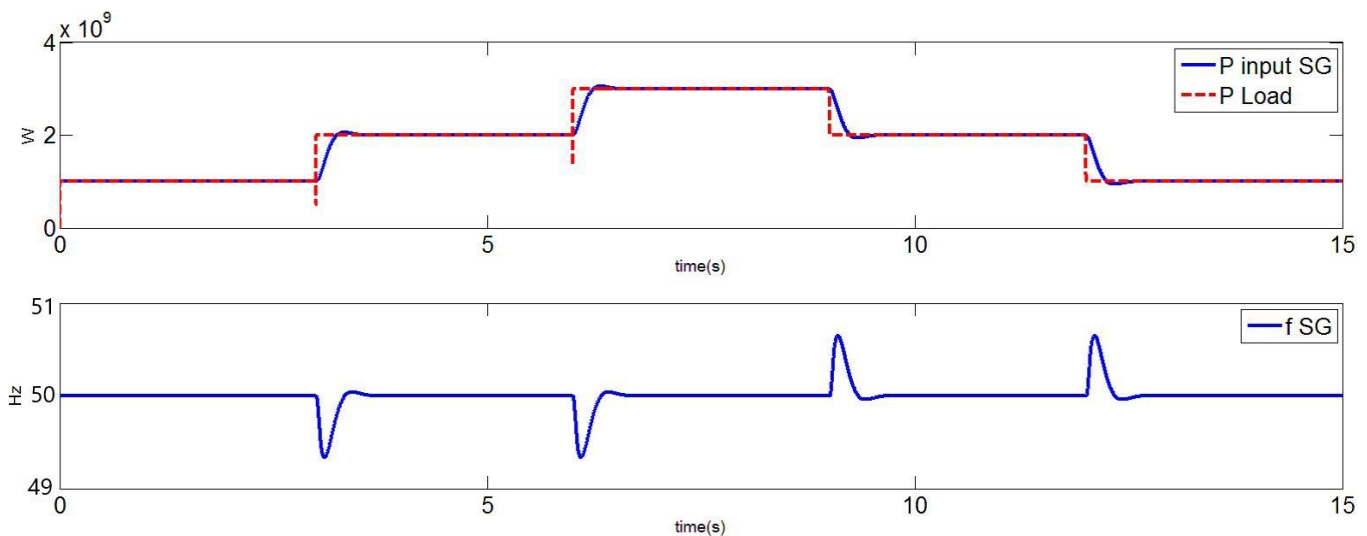


Figure 3.2.3 Secondary control of SG (system frequency and active power input of SG) [16]

As can be seen, the active power input is changed to be equal to the active power load. Furthermore, one observes that the frequency of the SG converges to the nominal, 50 Hz due to the change in active power input. This demonstrates the secondary control of an SG with regards to active power [16].

3.3 Synchronous Generator's Inherent Stability Mechanism

The Theory or Equations That Are Exploited In Synchronous Generator Control

It is very important to discuss the inherent properties of a SG that have enabled the synchronous generator play a significant role in power system operation and stability. They are namely: the inertia due to rotating masses, damping effect due to damper windings and active power-frequency (P-f) droop characteristics for load sharing. In this project, we seek to emulate this mechanism (represented by mathematical equations) in the control of a power electronic converter, a voltage source inverter (VSI) to be specific. As result of these properties, SG units contribute to the primary frequency regulation as well as voltage control or reactive power flow (through rotor excitation controls).

Inertia Due to Rotating Masses (J) and Damping of oscillations (D)

As the SG rotates, the field and damper windings of the rotor generate a sinusoidal flux in the air-gap, which consequently creates an emf in the armature terminals. The equation of motion of the rotor during disturbances in power networks is given by;

$$J \frac{d\omega_m}{dt} + D_d \Delta\omega_m = \tau_m - \tau_e \quad (3.3.1)$$

J – Moment of inertia of rotating masses (turbine and rotor), ω_m – angular speed of the rotor, ω_s – synchronous speed, $\Delta\omega = \omega_m - \omega_s$, τ_m - the mechanical torque, τ_e - electromagnetic torque and D_d – damping torque coefficient.

This equation is also known as the swing equation, as it describes rotor angle swings during disturbances in power networks. As seen, the swing equation captures the rotational inertia and damping of oscillations property of an SG.

The rotating mass provide inertia property (J) to the system frequency and the output of the synchronous machine. A simulation run on a 7th order synchronous machine model created in MATLAB for a 600MW power system load with different inertia facing a 20% load change, revealed that rotational

inertia (J) minimizes the frequency overshoot and provide a slower frequency response (6 times lower overshoot and around 10 times slower changing rate) [20].

Damping (due to mechanical losses) of rotor is small and can be ignored for all practical purposes [8]. In the event of small disturbances, the generator rotor experiences speed deviations and the damper winding helps in the restoration of the rotor synchronism. The response of a generator to a power system fault is analysed by breaking the entire fault period into three stages namely, sub-transient, transient and steady state. The damping effect is reflected in the transient state only. In the transient state, whenever the rotor speed (ω) is different from the synchronous speed (ω_{sm}), a **damping torque** is produced which according to Lenz's law tries to restore the synchronous speed of the rotor. Damping power (P_D) is given by $D_d \cdot \Delta\omega$.

Speed-droop Characteristics for Load Sharing

This section seeks to demonstrate the speed-load dependence of SGs. This characteristic is synonymous to the P-f droop characteristic explained in (primary control). This is because under steady state condition, the rotor speed in rev/min (N) of an SG is proportional to the frequency of the terminal voltage (f_e), this is given by;

$$N = \frac{120 \times f_e}{P} \quad (3.3.2)$$

Where; P is the number of poles

Both characteristics are effective because of the rotational inertia and damping property of the SG.

This implies that in the event of power imbalance between the input mechanical power to the generator and the electrical output to the grid, the rotor speed will change. The P-f droop characteristics couple output power with the rotor's rotating speed. For example, when there is a sudden increase in load resulting in a generation deficit, the rotor speed and system frequency decreases. But when the ALFC operates to increase the mechanical power input to the prime mover, the rotor speed increases and the output power of the SG increases to balance the system load.

The speed-load relationship of SGs connected in parallel can be represented by the following curve.

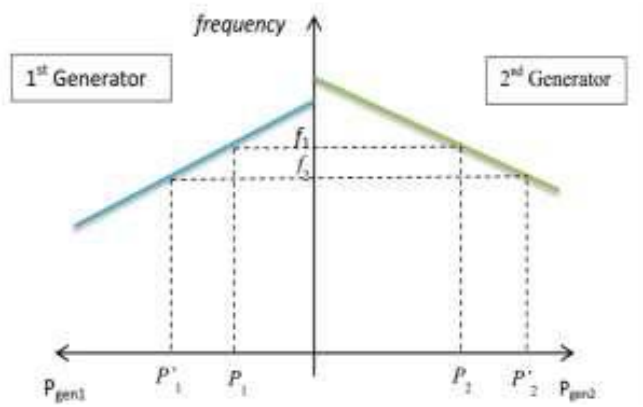


Figure 3.3.1 Speed-droop characteristics of a SG

When two generator units operate in parallel in islanded mode, they operate at the same frequency f_1 as shown in the diagram. If the load in the system increases remarkably, the additional load is shared according to the droop settings of the two generator and their frequency will change to f_2 . Nonetheless, substantial drops in frequency below a particular threshold values can pose danger to system components. Hence, in such cases, an adjustment of the governor reference (speed-changer setting) is required and that leads to a total generation increase of P_1' and P_2' [8], at the reference frequency, say 50Hz.

Synchronous machines have facilitated the stable operation of power systems for over 100 years, by providing load sharing and autonomous frequency regulation ability. Therefore, to guarantee the compatibility of millions of RESs with the grid, the inherent mechanism of SGs should be adopted as a rule of law.

3.4 The Proposed Solution – Virtual Synchronous Generator

Introduction

Now that the synchronous generator mechanism has been established, the idea of operating an inverter to mimic this SG mechanism connotes the virtual synchronous generator (VSG) concept. This concept is an attempt to introduce virtual inertia and damping in RESs through proper control of power electronic converters. This is to solve the stability issues created by high penetration of RES in the power grid. The main aim of this concept is to combine the dynamic characteristics of electromechanical SGs with the fast response of power electronic converters.

Background

Microgrids

Most renewable energy based DG units exist within microgrids. Therefore, it is important to know what a microgrid is. A microgrid (consisting of small-scale emerging generators, loads, energy storage elements, and control units) is a controlled small-scale power system that can be operated in an islanded and / or grid-connected mode, serving within a defined area to facilitate power supplementation and / or improved power quality to the consumer's premises [21]. It is a subset of LV or medium-voltage (MV) distribution networks (4 kV to 35kV phase to phase). The ratings of DG units usually range from 10 kW to 100 MW.

For the grid connected operation, the aim of the inverter would be to export controllable power with established voltage. However, in islanded operation, the lack of grid utility supply to a microgrid necessitates establishing the reference voltage and frequency. Therefore, DG units operated in an islanded microgrid are responsible for ensuring the reference voltage and frequency, which are the main functions of the inverter [21].

Two main control methods for power converter-interfaced units

There are two principal operations of inverters in microgrid operation: grid-following and grid-forming. The grid-following (GFL) mode, sometimes called grid-feeding and PQ control [21] is achieved by current source inverters (CSIs). For grid-forming (GFM) operation, voltage source inverters (VSIs) are usually employed to control the voltage and frequency of a network. The difference between the grid-following and grid-forming is that the former regulates their power output by measuring the angle of the grid voltage using a phase-locked loop [22]. Hence, they merely follow the grid angle/frequency and do not actively control their frequency output. In contrast, a grid-forming source actively controls its frequency and voltage output. Droop control is widely used in the GFM inverters to obtain frequency and voltage commands from measured real and reactive power values respectively [22]. Also, the GFL would need at least one grid former, i.e. a synchronous generator or a controlled voltage to be able to operate.

An islanded microgrid with a grid-forming inverter operation was chosen for our simulation since it is most suitable to demonstrate the P-f droop and Q-v droop characteristics emulation of synchronous generators in power electronic generators. This affords us the chance to set our own reference values for system voltage and frequency and then control each of these parameters using droop control with the swing equation or virtual inertia (similar to the SG).

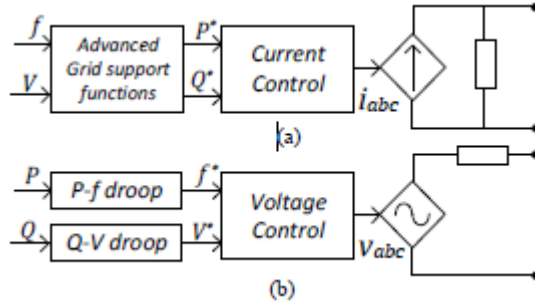


Figure 3.4.1 Inverter Controllers (a) Grid-following (GFW) control with grid support functions; and (b) Grid-forming (GFM) droop control [22]

3.4.1 The General Structure of the Virtual Synchronous Generator (VSG)

The VSG consists of energy storage, inverter and a **control mechanism** that controls power exchange between the energy storage and power system. It is usually located between a DC source and the grid. The energy storage device could be a battery, capacitor or flywheel. The power exchange supports the power system by preventing fluctuations similar to the SG rotational inertia. The **DC source** connected to the VSG algorithm emulates the SG's function by providing inertia and damping supports to the grid system. The **DC/DC converter** enables the VSG to absorb or inject (charge or discharge) power into the system from the energy storage device. The **inverter** is controlled to give output voltage and output frequency.

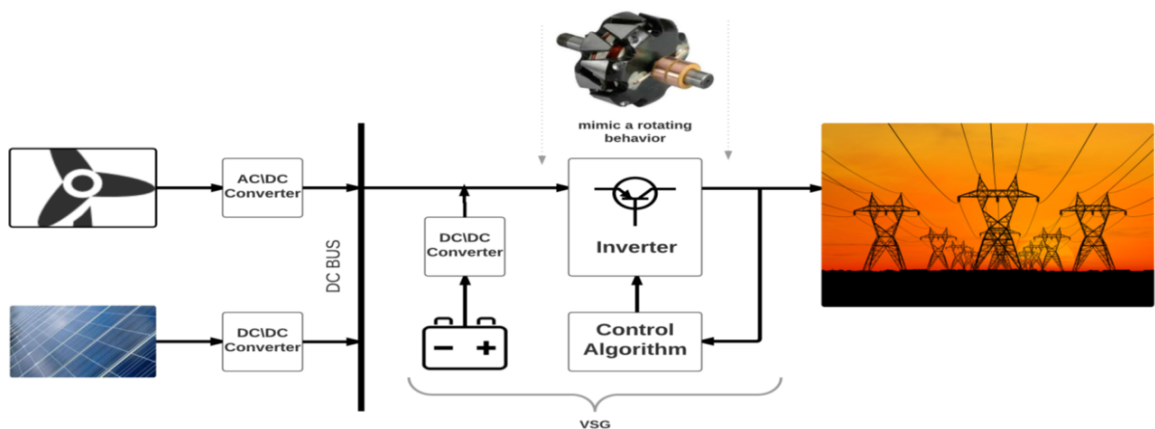


Figure 3.4.2 General structure of the VSG [19]

VSG application is an approximately a direct mathematical model of a SG. Depending on the required extent of complexity and accuracy in replicating the SG dynamics, the transient and sub-transient dynamics

of an SG model can be added or ignored [8]. Moreover, parameter selection for VSG applications is not restricted by the physical design of any conventional SG model, consequently, the VSG parameters can be chosen to mimic a particular behaviour of SG model or can be defined in the course of control system development to obtain the required characteristics [8].

Different control algorithms exist for VSGs though they possess the same general structure. Aside from the high frequency noise due to switching of inverter's power transistors [19], there is no difference between the electrical appearance of an electro-mechanical SG and the electronic VSG from the grid point of view.

3.5 The Proposed (Specific) VSG Control Algorithm

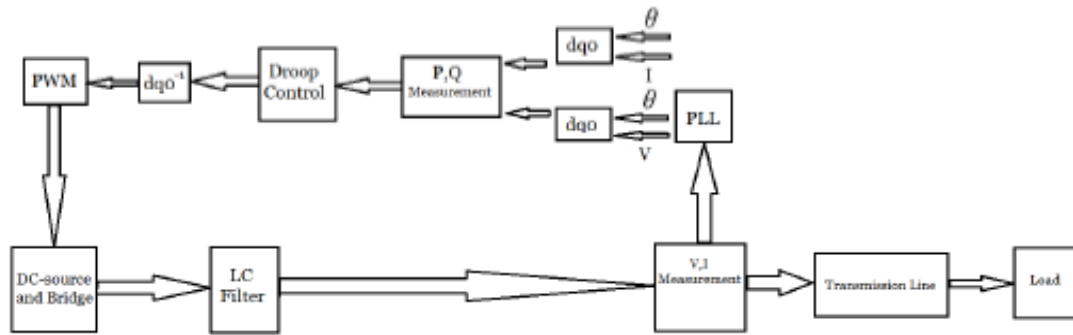


Figure 3.4.3 Proposed Algorithm - Overview of the VSG control system for an Islanded Microgrid

Overview of VSG Control System

A brief overview of the entire VSG control algorithm is presented and later the mathematical model of each element that emulates the synchronous generator is described. Other system components would also be explained in far greater detail.

The **DC source** is the primary source of energy in the microgrid. It is connected to a 3 phase inverter that converts the DC power to AC at 50 Hz. The droop controller consists of a **P-f** and **Q-v droop** controllers, a **voltage** controller and **current** controller. The **P-f droop controller** computes the phase angle (ωt) and the frequency of the VSG. The **Q-v droop controller** computes the reference voltage. The **voltage controller** is used to determine the reference current for the current control block. The **current controller** computes the 3 phase reference voltage for the pulse width modulation (PWM) generator. The P-f and Q-v droop controllers are simply **proportional controllers**, while both voltage and current

controllers use **proportional-integral (PI) controllers**. The **PWM generator** delivers the gate pulse to the inverter to provide the desired real and reactive power. The **LC filter** minimizes harmonics of the inverter output and helps in regulating the shape of the output voltage signal.

The **PLL** is used to determine the frequency and phase angle (ωt) of an incoming signal, in this case three phase voltages. The (ωt) is then used as the input for the so called **dq0 transformation**. Measured 3 phase voltages and currents are transformed from the ‘abc’ system to the ‘dq’ quantities and vice versa using **abc-dq0** and **dq0-to-abc** transformation blocks respectively. This concept is also known as the **Park’s transformation**.

Mathematical Model of Elements that emulate the Synchronous Generator

Active Power-Frequency (P-f) Control (with Swing Equation)

This system emulates the active power-frequency (P-f) droop characteristics (K_p), damping of rotor oscillations (D) and rotational inertia (J) of the SG.

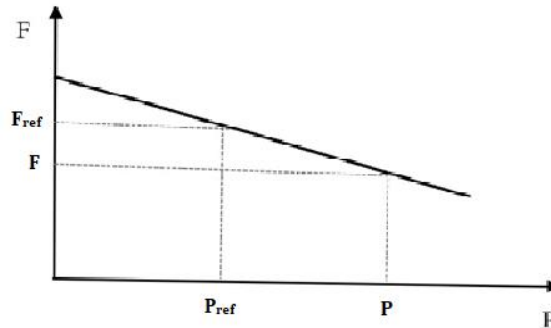


Figure 3.5.1 Active power-frequency relation

The P-f droop characteristic of the VSG is expressed as;

$$F = F_{ref} + K_p(P_{ref} - P) \quad (3.5.1)$$

K_p is also the slope of the graph above

K_p – P-f droop coefficient, F – frequency of the VSG, F_{ref} – reference grid frequency (50 Hz), P – measured 3 phase active power, and P_{ref} – is the reference real power.

The swing equation is utilized to emulate the inertia and damping property of the SG. By utilizing the swing equation;

$$P_{in} - P_{out} = J\Delta F' + D\Delta\omega \quad (3.5.2)$$

$$P_{in} = P_{ref} + \frac{(F - F_{ref})}{K_p} \quad (3.5.3)$$

$$\frac{1}{s} \left(\frac{P_{in} - P_{out} - P_D}{J} \right) = F \quad (3.5.4)$$

$$P_D = D(\omega_{VSG} - \omega_{ref}) \quad (3.5.5)$$

J – Inertia coefficient, **D** is the damping coefficient, **P_{in}** - input power from the voltage source, **P_{out}** - output power of VSG, **P_D** is the damping power

Equations 3.5.1, 3.5.2, 3.5.3, 3.5.4 and 3.5.5 are used in designing the P-F Droop control block diagram.

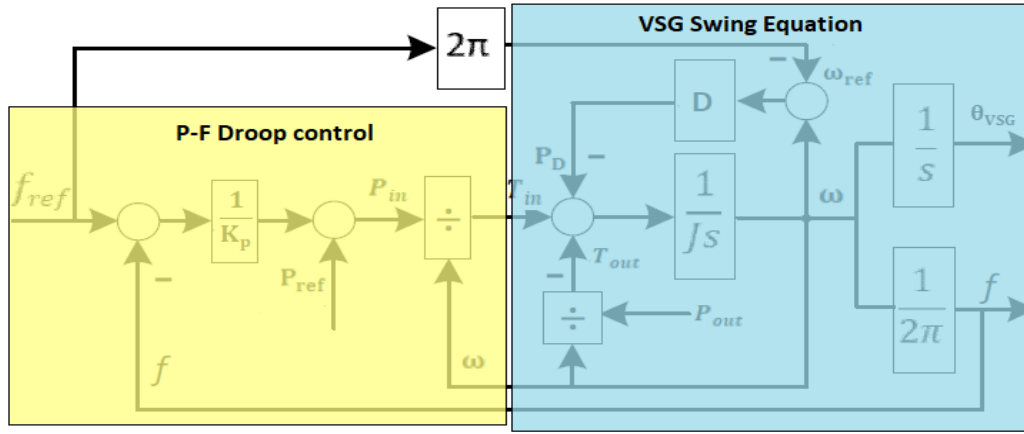


Figure 3.5.2 P-f droop control scheme with Swing Equation

Significance: **J** reduces the **maximum deviation of frequency** and gives a **smaller ROCOF** following a disturbance. Also, **D** helps to **weaken fluctuations** and then decrease the **settling time** of the frequency.

Reactive Power-Voltage (Q-v) Droop Control

This system emulates the reactive power control (**K_v**) of the SG.

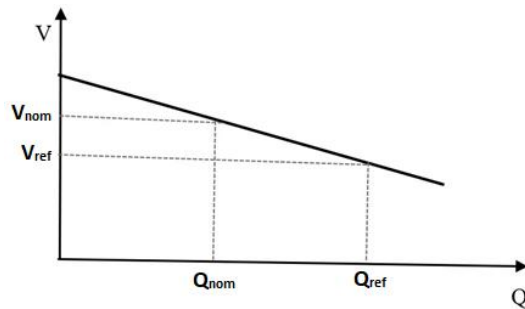


Figure 3.5.3 Reactive power-voltage curve

The Q-f droop characteristic of the VSG is expressed as;

$$V_{ref} = V_{nom} + K_v(Q_{nom} - Q_{ref}) \quad (3.6.1)$$

K_v - Q-V droop coefficient, V_{ref} – output voltage of the Q-V droop controller, V_{nom} - nominal grid voltage, Q_{ref} – measured 3 phase reactive power, and Q_{nom} is the nominal reactive power

Equation 3.3.2 is used in designing the Q-v Droop control block diagram.

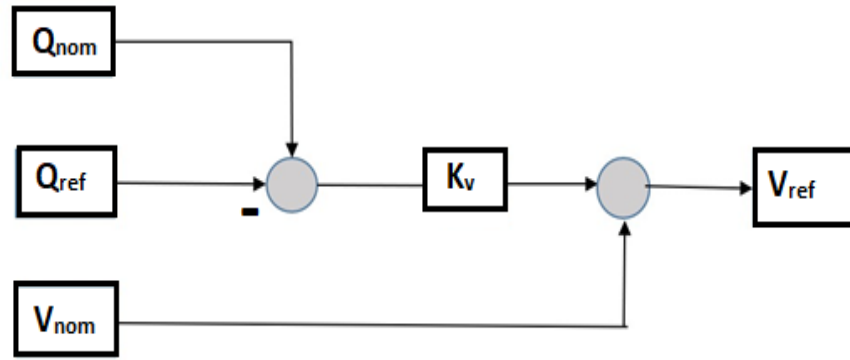


Figure 3.5.4 Reactive power-voltage droop control scheme

Significance: The Q-v droop control gives voltage regulation ability to the VSG. (Voltage stability)

STUDY OF THE OTHER SYSTEM COMPONENTS

Voltage and Current Controllers

Voltage Control

The aim of voltage control is to compute the reference current value for the inverter output.

Using Park's Transformation the following equations result

$$(E - V_{gd}) \left(K_{vp} + \frac{Kv_i}{s} \right) = I_{dref} \quad (3.7.1)$$

$$(-V_{gq}) \left(K_{vp} + \frac{Kv_i}{s} \right) = I_{qref} \quad (3.7.2)$$

Where E – Q-v droop controller reference output voltage, I_{ref} – reference current values for the current controller, V_g – grid voltage, where K_{vp} and Kv_i are the proportional and integral gain, respectively. Proportional-Integral (PI) controllers are used in other to make the output voltage track the reference values.

According to equations 3.7.1 and 3.7.2, the voltage control loops is shown in Figure 4.6, where K_{pv} and K_{iv} are proportional and integral gains in the PI controllers.

Current Control

It is assumed that the LC filter is lossless. Then, the dynamic equation of voltage (AC side) of the inverter can be expressed as

$$Li' = V_{inv} - V_{grid}$$

Where L is the filter inductance, V_{inv} is the inverter output voltage, and V_{grid} is the measured grid voltage and i is the current through the inductor. Using Park's transformation, the filter equation can be expressed as:

$$Li'_d = V_{invd} - V_{gridd}$$

$$Li'_q = V_{invq} - V_{gridq}$$

A PI controller is used in order to make the output current track the reference current. The reference voltages obtained in the dq0 frame are converted to reference values in the abc frame using the inverse Park's transform. These three-phase reference voltages, are then used as the main driver for the PWM block, which will control the inverter by providing the gate pulse, ensuring the desired output.

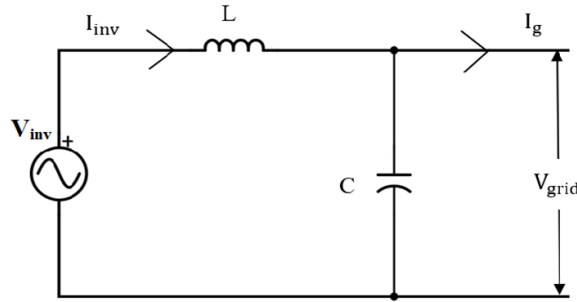


Figure 3.6.1 Grid side of LC filter

$$V_{invd} = V_{gridd} + \left(\beta_p + \frac{\beta_i}{s}\right)(I_{dref} - I_d) \quad (3.7.3)$$

$$V_{invq} = V_{gridq} + \left(\beta_p + \frac{\beta_i}{s}\right)(I_{qref} - I_q) \quad (3.7.4)$$

In other to make the output current track the reference current, Proportional-Integral (PI) controller is used, where β_p and β_i are the proportional and integral gain, respectively.

Equations 3.7.3 and 3.7.4 are used to design the current controller in Figure 4.6.

LC Filter

The LC filter consists of an inductor in series with a capacitor in parallel with the grid. Their impedances are denoted by Z_1 and Z_2 as seen in Figure

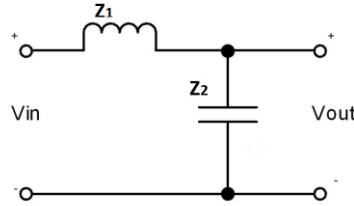


Figure 3.6.2 LC-Filter

$$\frac{V_{out}}{V_{in}} = \frac{Z_2}{Z_1 + Z_2} \quad (3.8.1)$$

$$\frac{V_{out}}{V_{in}} = \frac{1}{LCs^2 + 1} \quad (3.8.2)$$

If $V_{out} = V_{in}$, then equation can be written as $f = \frac{1}{2\pi\sqrt{LC}}$ (3.8.3) , where f is the cut off frequency, in our case 1000 Hz has been chosen.

The 3 phase Inverter and PWM technique

The 3 phase (bridge) inverter consists of six switching devices such as IGBTs or MOSFETs with each connected to an antiparallel diode. The bridge may use a PWM signal as the gating signal. The PWM generator outputs a total of six pulses (per cycle), two for each pulse. For a particular phase, whenever the signal for the upper device has a value of 1, the lower would have a value of 0 and vice versa. This is to prevent short circuit occurrence.

The PWM signal is generated by comparing an input signal (modulating signal) with a triangle carrier function. Whenever the input signal has a value that is higher than the carrier function, the output is 1 and whenever the input is lower than the carrier function the output is 0. The carrier frequency is specified, usually much higher than the frequency of the grid so it does not negatively influence the load.

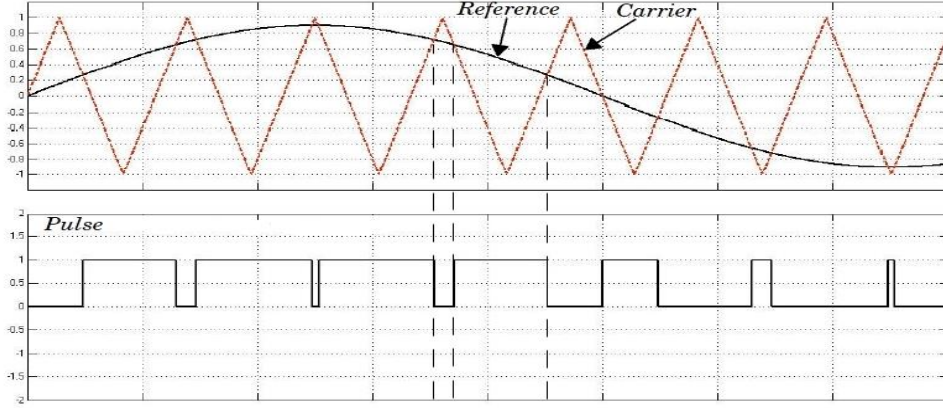


Figure 3.6.3 Pulse modulation by comparing the reference signal to the carrier signal

The pulse width is adjusted in order to vary the average output value of the inverter. Thus, the larger the width the higher the average value. While, the number of pulses within a cycle affects the output frequency. Thus, the more the number of pulses the higher the output frequency. Therefore, the PWM signal is generated from a control algorithm to give desired output voltage and frequency.

Dq0 Transformation

In the dq0 frame, the time-dependent coefficients are eliminated. This makes it possible to independently control the active and reactive power flows. The output power of the VSG is estimated by the grid-side voltage and current and is given by;

Active Power:

$$P_{out} = U_d I_d + U_q I_q \quad (3.9.1)$$

Reactive Power:

$$Q_{out} = U_q I_d - U_d I_q \quad (3.9.2)$$

Where the $U_{d,q}$ and $I_{d,q}$ are the dq0 sequences of the grid voltage and current.

4. METHODOLOGY & IMPLEMENTATION

4.1 Introduction

In this chapter, the model of two test cases are presented to evaluate the proposed closed-loop control of the voltage source inverter (VSI) in grid-forming islanded microgrid operation. The first case is an uncontrolled microgrid model while the second case is our controlled microgrid model. The two test cases would help to investigate the effectiveness of our design and the scope for improvement in design. Also, the methods used in determining some design parameters are explained.

4.2 Methodology

Case Study A: Uncontrolled System

A three-phase inverter with pulse-width modulation (PWM) as gating in an islanded microgrid was modelled without closed-loop control. This demonstrates the general behaviour of an uncontrolled inverter when subjected to changes in load or other disturbances in a RE based DG unit.

Case Study B: Controlled System (P-f droop control, Q-v droop control and Rotational Inertia emulation of SG)

A three-phase inverter with closed-loop control for islanded operation is modelled. This demonstrated the P-f droop and Q-v droop characteristics emulation of an SG as well as the rotational inertia emulation of an SG. Hence, the dynamic response of the controlled system to changes in load and other disturbances was evident.

4.3 Implementation

Model of the Uncontrolled System (Case A)

Here, an uncontrolled inverter supplying power to three sets of loads. Load 1 remains in circuit throughout the simulation period. Load 2 and 3 are switched either on or off in the course of the simulation. The power source for the inverter is a constant DC voltage source (1.94 pu), and PWM technique was used to regulate the inverter. There was no control mechanism to regulate the voltage, current and frequency of the inverter.

A fixed modulating signal is applied to the PWM, with modulation index of **0.85**. The loads are connected through an LC filter to remove the inverter ripple current. The AC frequency output of the inverter is **50** Hz, and the switching frequency is **2000** Hz. Since this is the uncontrolled system, only resistive loads were considered.

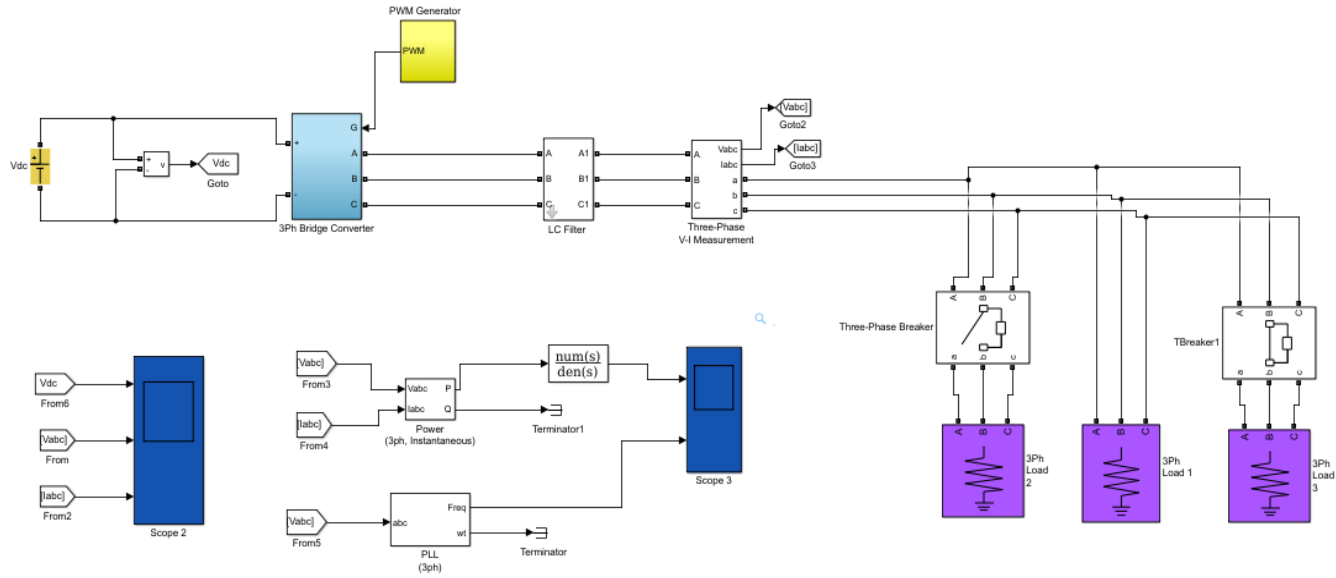


Figure 4.1 Simulink Design Diagram for Case A

The purpose of this case study is to investigate the uncontrolled system dynamics and thereby determine areas of improvement. The DC voltage in this design was. Load 1 was on the grid side. Thus, the desired line voltage was which corresponds to a (peak) phase voltage of 1.0 pu, and desired output rms current of 1.263 pu. The base values of voltage, current and frequency used for all simulations are 380 kV, 3645 A and 50Hz.

Parameters for modelling Case A

LC Filter Design – Since the carrier frequency (f_c) was 2000Hz and harmonics occur at multiples of f_c , the cut off frequency was taken to be **1000Hz**. The filter inductance was chosen to be **0.27mH**. Hence, the filter capacitance C can be calculated below.

$$C = \frac{1}{L \times (2\pi f)^2} = \frac{1}{0.27 \times 10^{-3} \times (2\pi \times 1000)^2} = \mathbf{93.8\mu F}$$

Table 4.1 Parameters for Simulation of Case A

Islanded Microgrid Parameters:	V_{dc}	L (filter)	C (filter)	Carrier frequency
	1.93 pu	0.27 mH	93.8 μ F	2000 Hz

Model of Controlled System (Case B)

For Case B, a droop controller together with inertia emulation has been introduced to regulate grid frequency and inverter output voltage with changes in load. As discussed in chapter 3, the proposed virtual synchronous generator along with voltage and current controllers is used to generate the reference signals for the PWM. But in this case, a space vector PWM (SVPWM) is employed. For performance evaluation, the same load switching patterns in Case A were used. I.e. The following scheme provides an overview of our system model using the MATLAB Simulink:

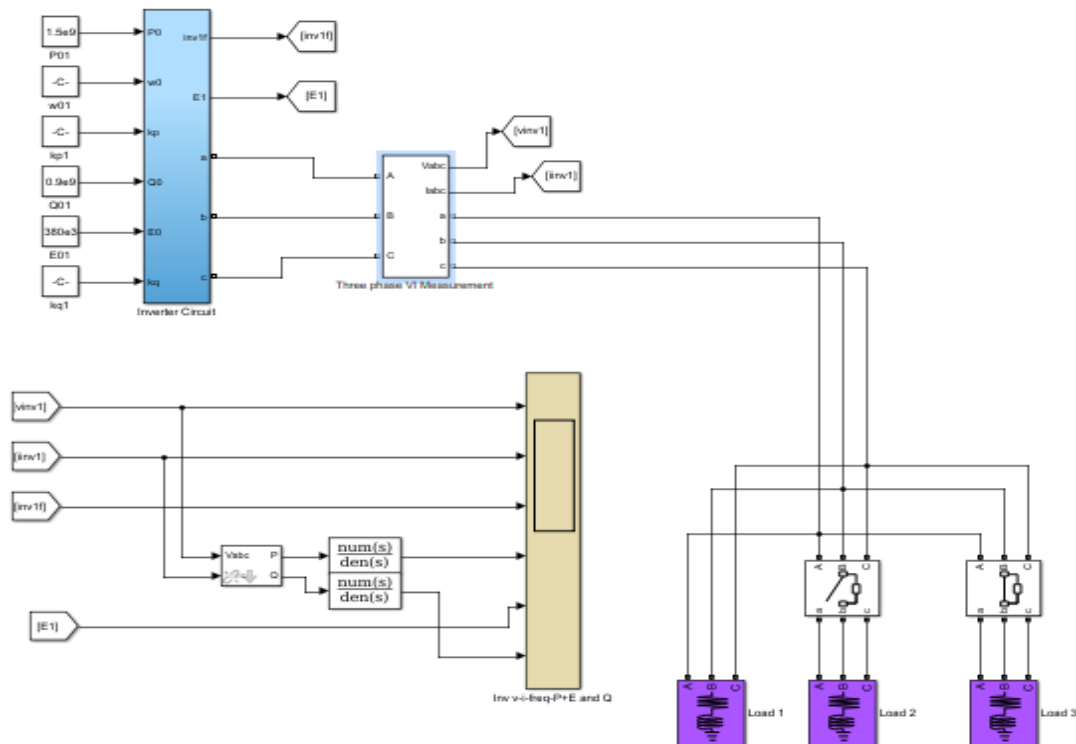


Figure 4.2 Simulink design diagram of controlled inverter in an island microgrid

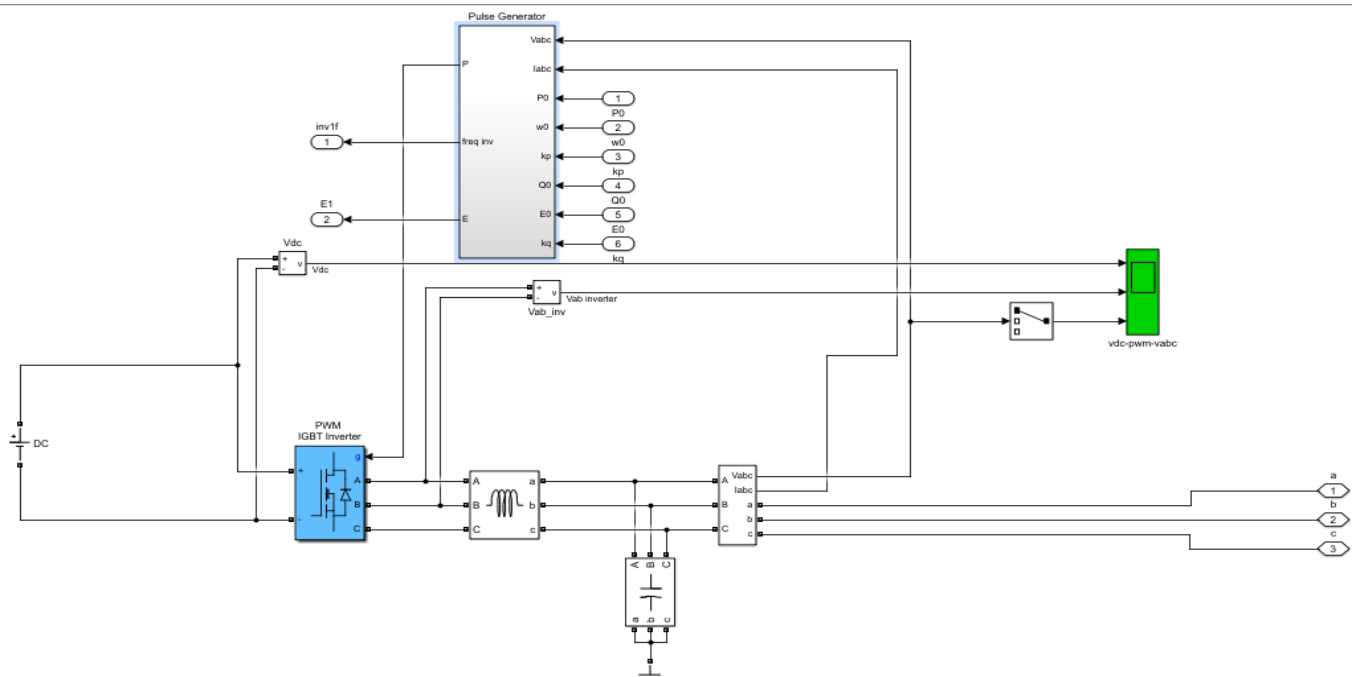


Figure 4.3 Inverter circuit block in Figure showing 3 ph. inverter, LC filter and Pulse generator block

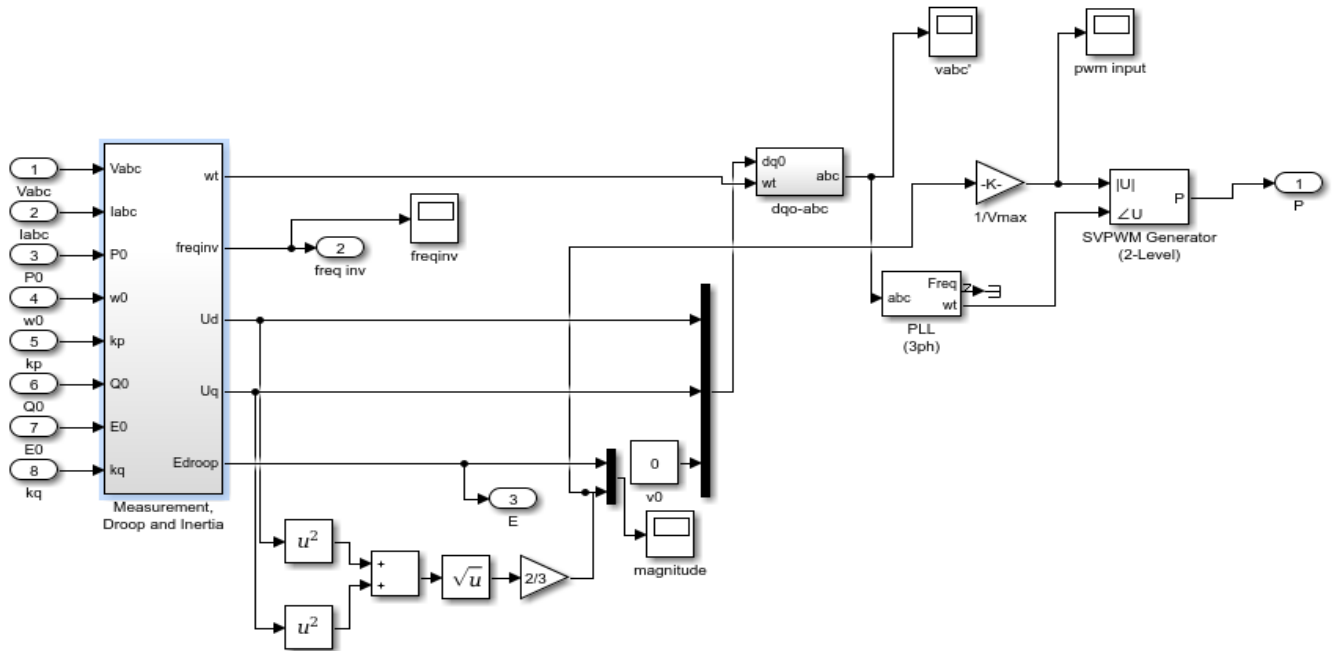


Figure 4.4 Pulse generator block in Figure showing the SVPWM generator and the Measurement, Droop control and Inertia emulation block

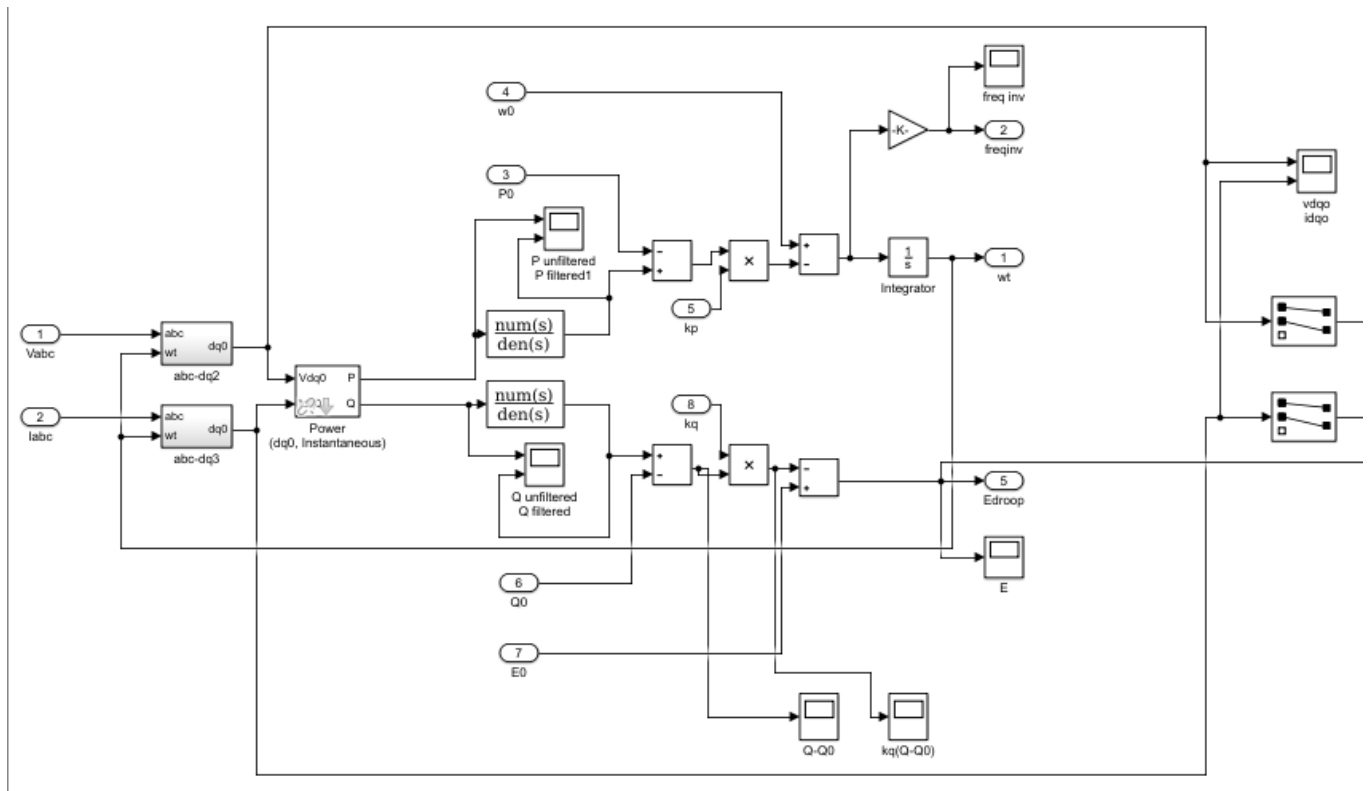


Figure 4.5 Power measurement, P-f and Q-v droop control, and Inertia Emulation

Droop Controllers Design – Proportional gains

$$\omega = \omega_0 - k_p (P - P_0)$$

$$K_p = \frac{\omega_0 - \omega}{P - P_0} = \frac{(50 - 49.9) \times 2\pi}{(2 - 1.5) \times 10^9} = 1.257 \times 10^{-9}$$

$$E = E_0 - k_q (Q - Q_0)$$

$$K_q = \frac{E_0 - E}{Q - Q_0} = \frac{(380 - 361) \times 10^3}{(1.2 - 0.9) \times 10^9} = 6.33 \times 10^{-5}$$

PI Controller Design

The proportional and integral gains of the PI controller were determined through tuning.

Table 4.2 Parameters for modelling Case B are summarised below.

Islanded Microgrid Parameters:	V_{dc}	L (filter)	C (filter)	Carrier frequency
	1.63 pu	0.02 H	30 μ F	2000 Hz

Droop & Voltage Control:	K_p	K_q	K_{vp}	K_{vi}
	1.257×10^{-9}	6.33×10^{-5}	1	50

Current Control and Delay factor:	β_p	β_i	τ	
	1	50	0.01	

Droop Control	P_{ref}	Q_{ref}	F_{nom}	V_{nom}
	1 pu	0.6 pu	50 Hz	1 pu

5. RESULTS AND DISCUSSION

5.1 Introduction

This chapter presents the simulation results of the controlled and uncontrolled inverter under normal operation and changes in load (demand). Analyses are carried out on the results and the findings are discussed.

5.2 Simulation Results

Case A (Uncontrolled System)

Normal Operation

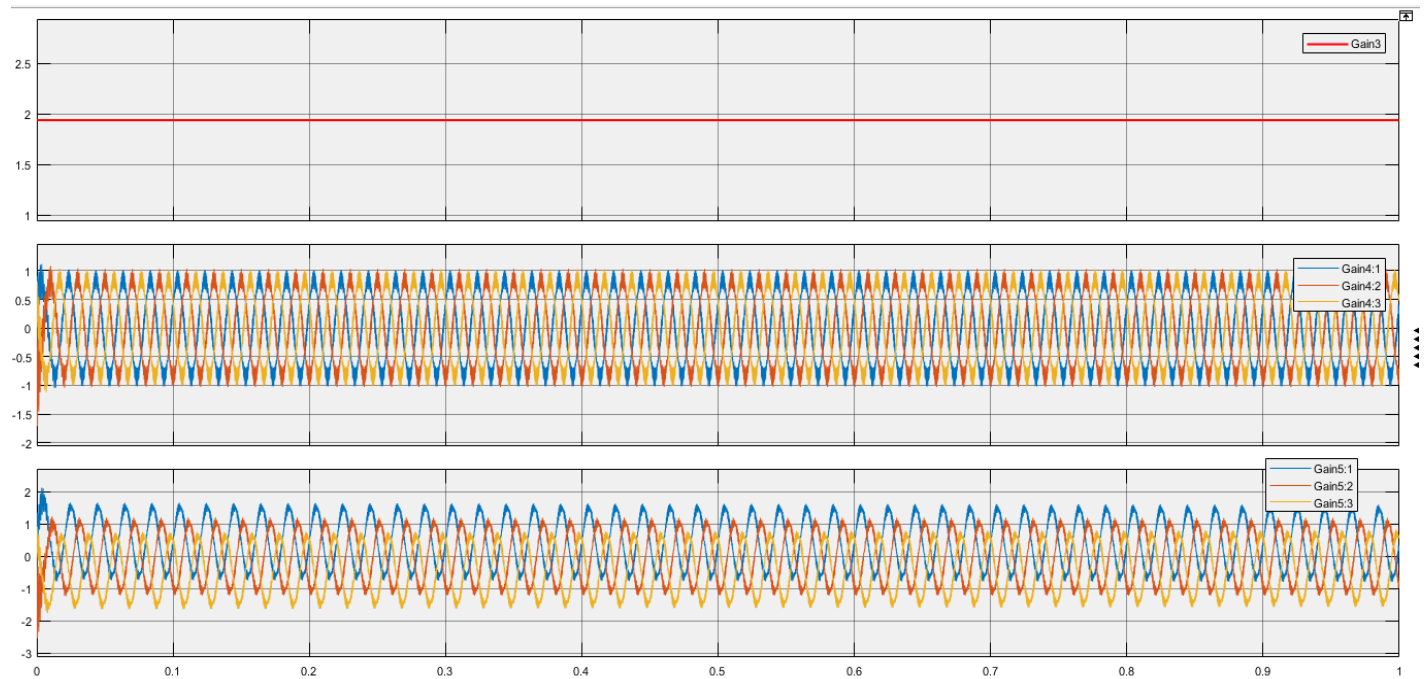


Figure 5.1.1 DC Voltage, System voltage and current for normal operation

Figures 5.1.1 and 5.1.2 show DC supply voltage, the system voltage, current, active and reactive power and frequency response under the normal condition without any disturbance in the system. Figure 5.1.2 shows sinusoidal signals of inverter as a result of filtering the harmonics. The peak system voltage is 1.008 pu. The three phase current signals have been displaced in magnitude due to the presence of reactive load. With the peak of the current signals been roughly 1.647 pu, 1.196 pu and 0.844 pu. Also, there are small amplitude oscillations in power and frequency response which may adversely affect the

system stability. This phenomenon implies the importance of the frequency and voltage control; if we can control the frequency and voltage, we will be able to control the real and reactive power.

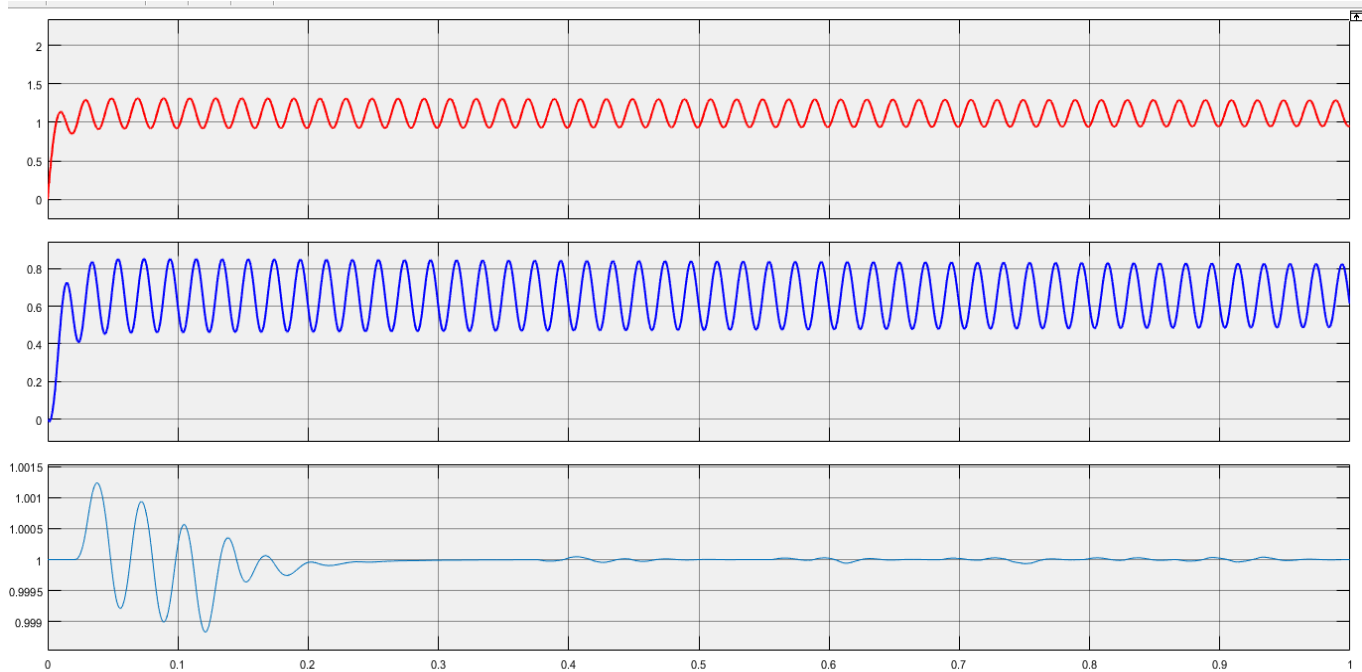


Figure 5.1.2 Active Power, Reactive power and system frequency for normal operation

Sudden change in the load side.

To observe the system response under a sudden disturbance from the load side, the three phase breaker connected to load 2 was closed from time $t = 0.3$ sec to 0.55 sec and that connected to load 3 was opened from $t = 0.9$ sec to 1.15 sec. Load 2 provided a 30% increase in load (both active and reactive power) while load 3 was opened to represent a 30% decrement in load (both active and reactive). All percentages are with respect to the base load.

Figures 5.1.3 and 5.1.4 show the DC supply voltage, the system voltage, current, active and reactive power and frequency response when these sudden changes occurred in the system. For both increase and decrease in load, the output voltage (system voltage) remains unchanged. However, the current reacts immediately to accommodate the change of load. However, the three current signals are displaced in magnitude as seen in figure 5.1.3.

Figure 5.1.4 shows frequency drifts due to change in load. When the load was increased at $t = 0.3$ s, the frequency drops precipitously but returning to the rated frequency after a short time. Also, when the load

was decreased at $t = 0.9\text{s}$, there was an immediate rise in frequency which returned to the rated frequency after a short time. The phase-locked loop (PLL) that was used to obtain the frequency signal was enabled to perform automatic gain control and hence might not give the accurate frequency response. These variations in frequency with changes in load suggest the need for adding droop controller in the system.

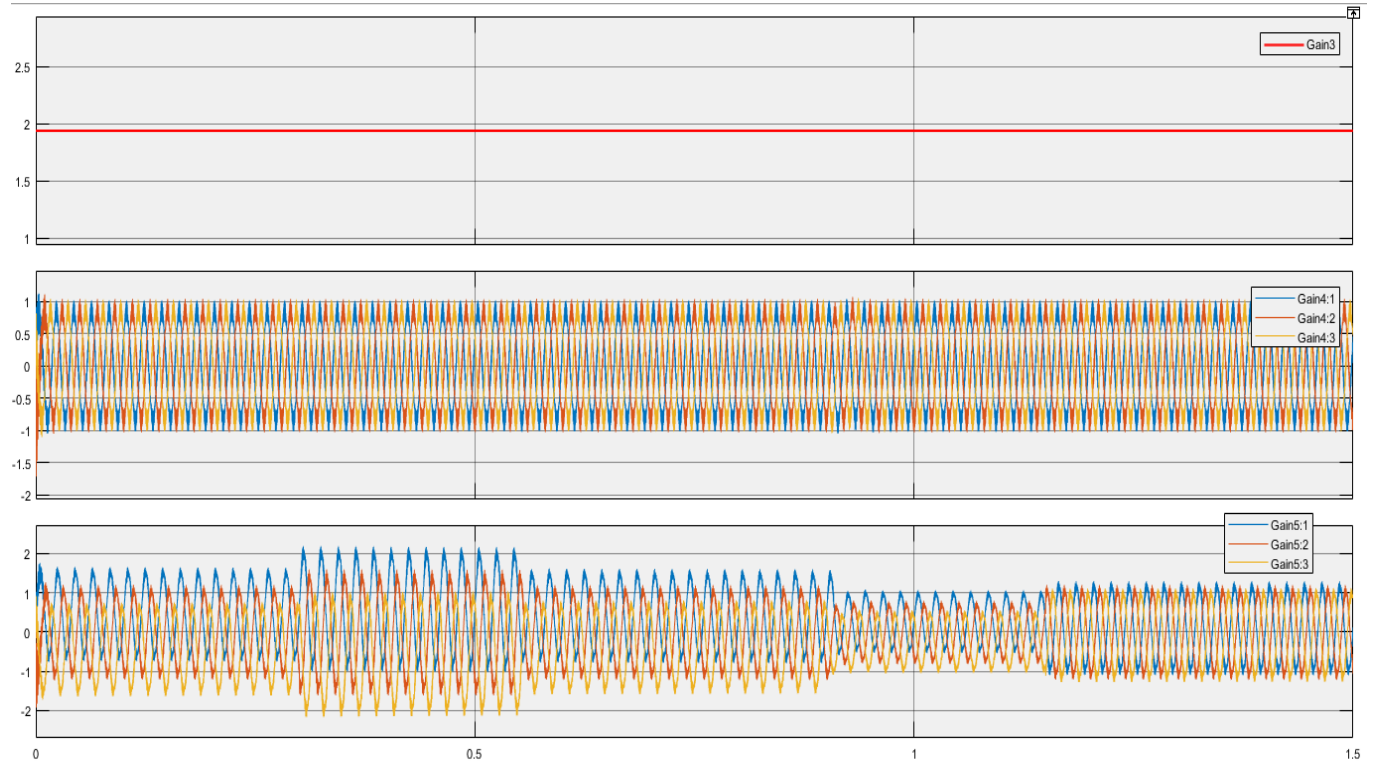


Figure 5.1.3 DC voltage, system voltage and current when an impedance load is switched on from $t = 0.3$ to 0.55 s and switched off from $t = 0.9$ to 1.15s .

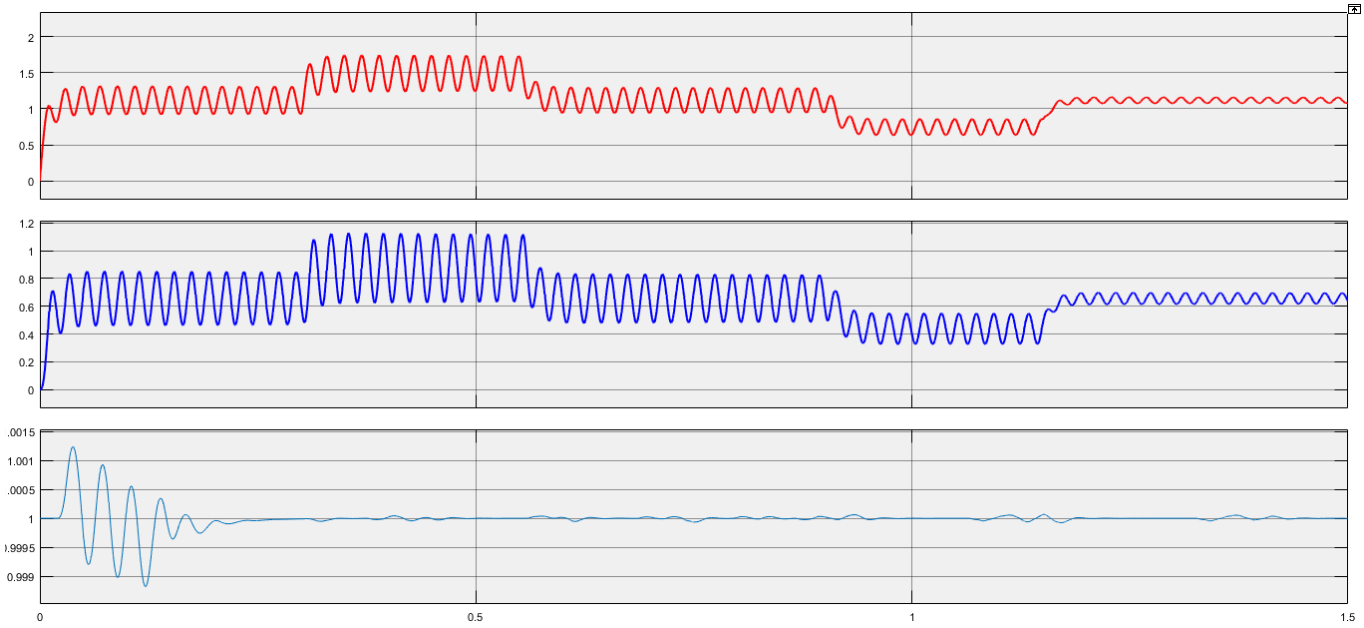


Figure 5.1.4 Active Power, Reactive power and system frequency when an impedance load is switched on from $t = 0.3$ to 0.55 s and switched off from $t = 0.9$ to 1.15 s.

Case B (Controlled System)

Normal Operation (Without any change in load)

The purpose of this experiment is to evaluate the established model of the voltage source based VSG in which a droop control and inertia emulation is implemented for the inverter. We ran the simulation with a base load ($1.0 + j0.6$ pu) under normal and disturbance situations. The input DC voltage is 1.63 pu. SVPWM was used for gating the inverter. The desired grid voltage was corresponding to approximately 1 pu (peak of phase voltage) and grid current of approximately 1.212 pu (peak). Simulation results for the base load under normal operation is shown in Figure 5.2.1

The load side voltage and current were measured as shown in figure 4.2. The measured power from the grid voltage and current were computed using a PQ measurement block. Figure 5.2.1 shows that the output voltage and current becomes sinusoidal as it passes through the LC filter. From the voltage plot, one can see that voltage signal peaks at roughly 0.978 pu, which corresponds to a rms value of approximately 0.671 pu and an output current of roughly 0.848 (rms). The system output voltage and current are slightly below the desired values which suggest that there is some loss of power.

The system frequency, active power, reactive power, and inverter reference output voltage are fairly constant throughout the simulation, with values approximately 50.03 Hz, 0.994 pu, 0.596 pu and 1.013

pu respectively. This represents an improvement over the uncontrolled system. The system power response in figure 5.2.1 suggests there is some loss of power which could be mainly due to the impedance as poised by the LC filter. From the above experiment, we can conclude that the proposed VSG control system is working properly for both reactive and real loads under normal operation.

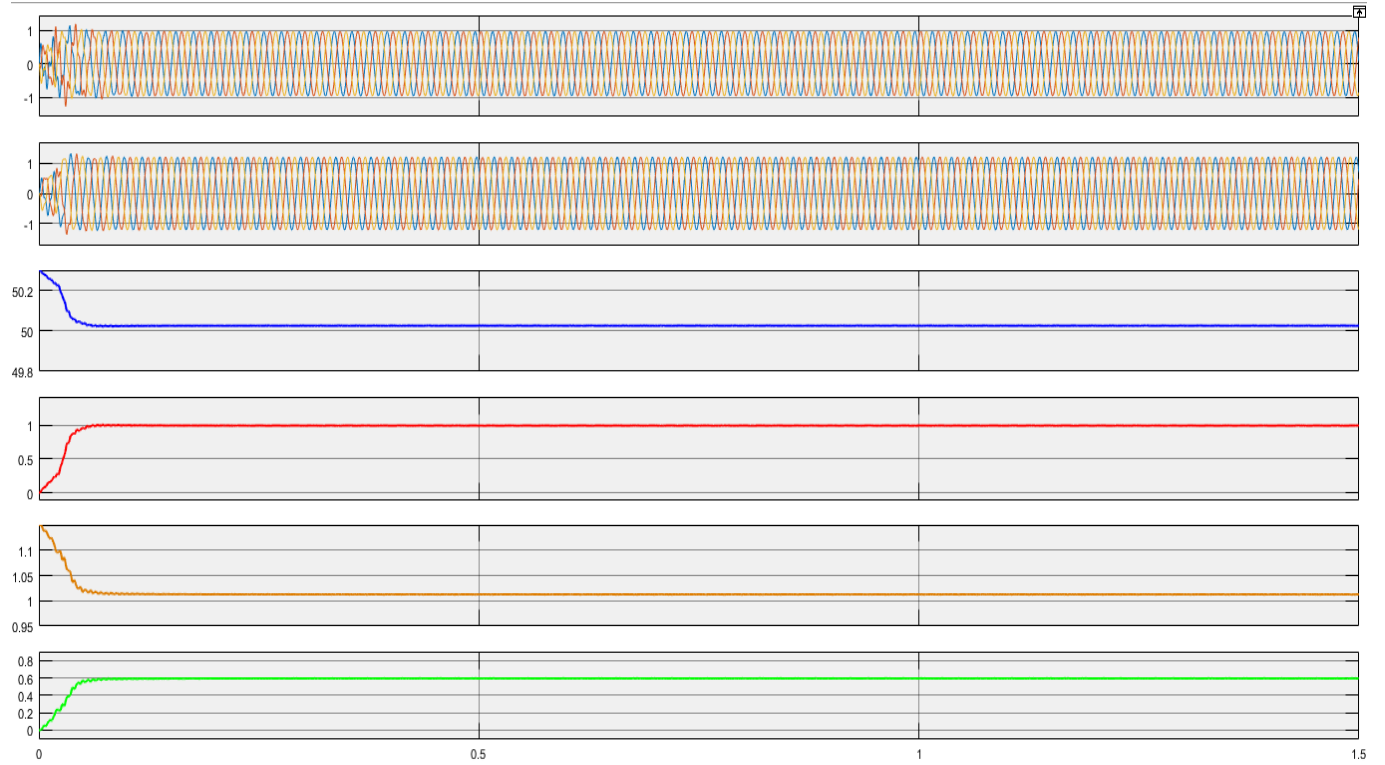


Figure 5.2.1 System voltage (V), current (I), frequency (f), Active Power (P), inverter reference output voltage (E) and Reactive power (Q) for normal operation.

Sudden change in load

Next, to observe the system response under a sudden disturbance from the load side, the three phase breaker connected to load 2 was closed from time $t = 0.3$ sec to 0.55 sec and that connected to load 3 was opened from $t = 0.9$ sec to 1.15 sec. Sudden changes are made to the base load. Firstly, the change in load was resistive only, and then reactive only and lastly, both resistive and reactive.

Change in active power (resistive load only)

Figure 5.2.2 shows the dynamic response of the system due to changes in real power in load side. Active power changed from approximately 1.021 pu to 1.352 pu at time $t = 0.3$ sec to $t = 0.55$ sec. Also, active power reduced approximately from 1.021 pu to 0.66 pu from $t = 0.9$ sec to 1.15 sec. Figure 5.2.2 demonstrates the voltage and current variation of the system due to the real power changes. When there the resistive load increases, the current response reacts immediately increasing from roughly 1.124 pu to 1.465 pu (peak) and decreasing from roughly 1.124 pu to 0.816 pu (peak) when the resistive load was decreased. However, in all these changes in resistive load, the bus voltage remains unchanged or had a very small change which is expected since the reference voltage in the VSG control has been set to maintain a constant 1.0 pu (phase voltage peak). Similar to practical generator excitation control system, in this proposed control system, Q-V droop controller provides voltage which remain same as nominal voltage during disturbances.

From Figure 5.2.2, one can see that real power is increasing while reactive power remains unchanged as expected. Most importantly during the disturbances, there is just a slight change in frequency, which remains fairly constant at 50 Hz to keep system stable. Just like the prime mover, the P-f controller here compensates the drop in frequency during disturbances with slight deviation. Using appropriate gain, it is possible to have improved frequency response during disturbances.

Compared to case A, there is a significant improvement in power and frequency response. However, negligible oscillations in power and frequency signals were observed. The above experimental results show that the proposed control system responds satisfactorily to changes in real power on the load side and kept the system stable. The inertia emulation (τ) prevented the abrupt change in frequency during the disturbances.

Change in reactive power (inductive reactance load only)

In this previous section, system stability due to change in real power was evaluated. In this section, the proposed control system as changes occur in the reactive load. To accomplish this, reactive power was changed from approximately 0.6 pu to 0.831 pu at time $t = 0.3$ sec to $t = 0.55$ sec. Also, reactive power reduced approximately from 0.6 pu to 0.408 pu from $t = 0.9$ sec to 1.15 sec. Figure 5.2.3 demonstrates this. When there the resistive load increases, the bus voltage decreases from approximately 0.895 pu to 0.846 pu and when reactive load decreases, the bus voltage increases from roughly 0.895 pu to 0.963 pu. For the conventional synchronous generators, terminal voltage is tightly coupled with reactive

power generation. Hence, we observe that the proposed VSG also shows this effect as the inverter output voltage decreases with increase of reactive power. However, oscillations are seen in the active and reactive power, the inverter reference output voltage and frequency except from $t = 0.9$ sec to 1.15 sec. The three phase current signals were also displaced in magnitude except from $t = 0.9$ sec to 1.15 sec.

Change in both real and reactive power

Lastly, we evaluate the characteristics of the controlled system due to changes in both resistive and reactive load. For this experiment, the base load is connected throughout the simulation period. Load 2 and 3 which are both rated $(0.5 + j0.3)$ pu are switched on and off from $t = 0.3$ s to 0.55 s and $t = 0.9$ and 1.15 s respectively. Figure 5.2.4 demonstrates the results of this experiment. The bus voltage or system voltage remains fairly constant throughout the simulation period. When there the load increases, the current response reacts immediately increasing from roughly 1.189 pu to 1.463 pu (peak) and decreasing from roughly 1.189 pu to 0.761 pu (peak) when the load was decreased. The inverter reference output voltage also decreases roughly from 0.594 pu to 0.409 pu for the increase in load and increases roughly from 0.594 pu to 0.77 pu for a decrease in the load. The system frequency decreases roughly from 50.02 Hz to 49.92 Hz for the increase in load and increases from roughly 50.02 Hz to 50.11 Hz for a decrease in the load.

Figure 5.2.4 thus demonstrates the active power-frequency (P-f) and reactive power – voltage (Q-v) droop characteristics of SG in the voltage source inverter (VSI). A change in active power produces an inversely proportional change in frequency. Similarly, a change in reactive power produces an inversely proportional change in inverter reference output voltage.

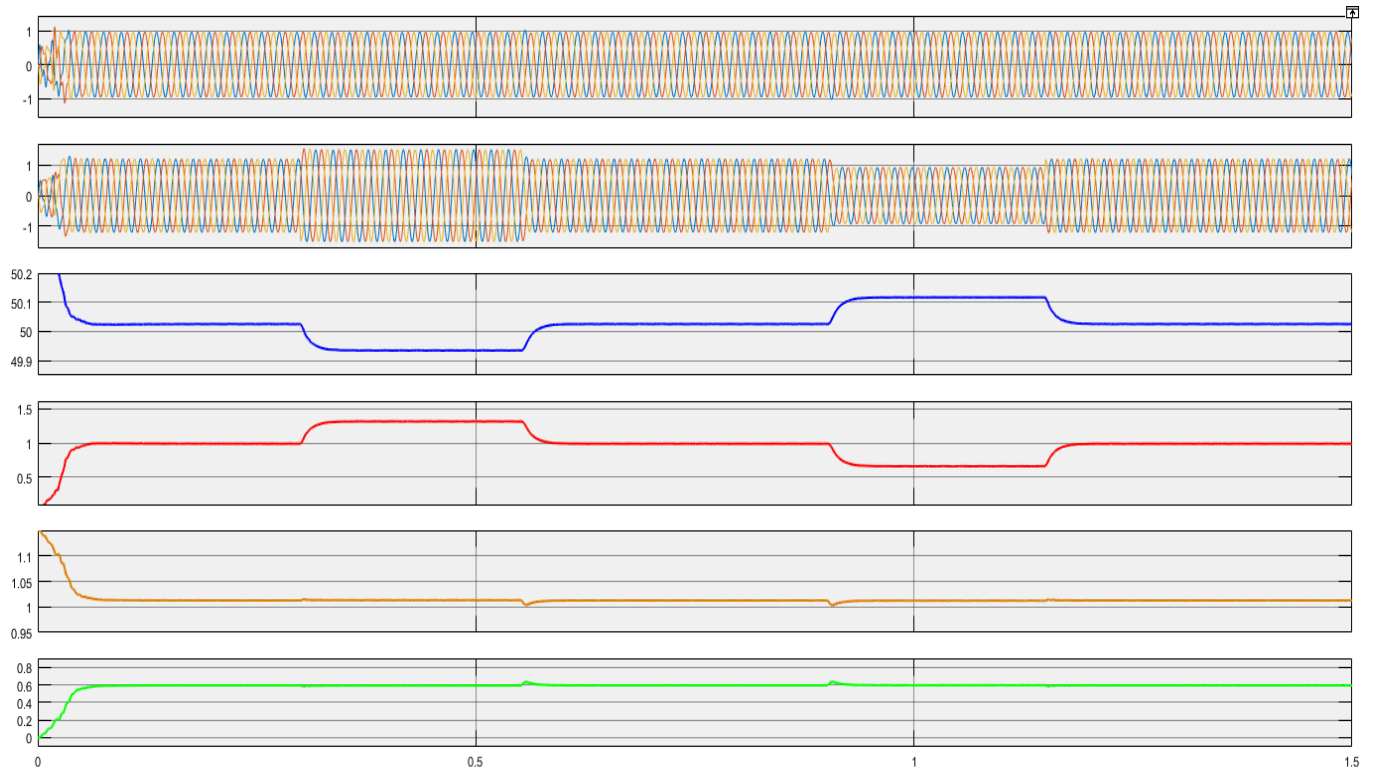


Figure 5.2.2 V, I, f, P, E and Q when a resistive load is switched on from $t = 0.3$ to 0.55 s and switched off from $t = 0.9$ to 1.15 s.

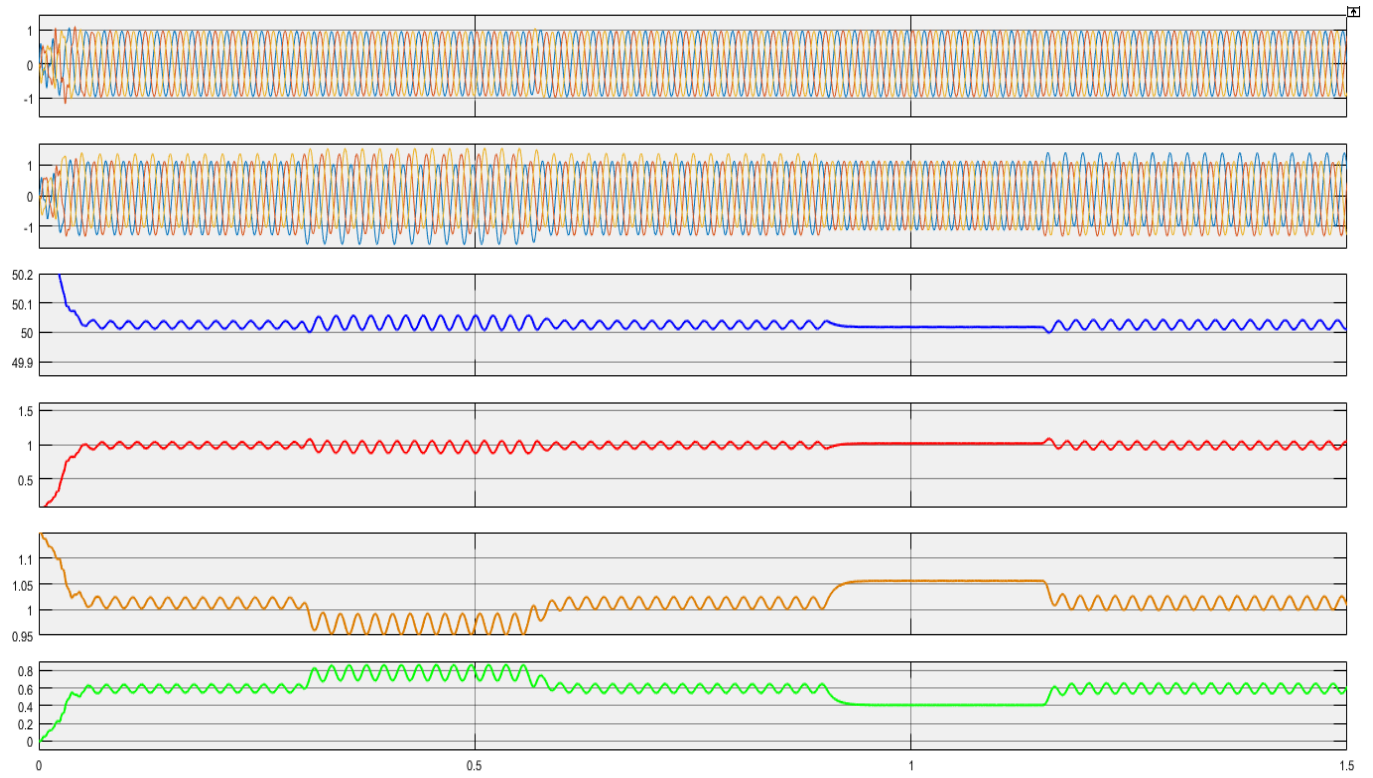


Figure 5.2.3 V, I, f, P, E and Q when a reactive load is switched on from $t = 0.3$ to 0.55 s and switched off from $t = 0.9$ to 1.15 s.

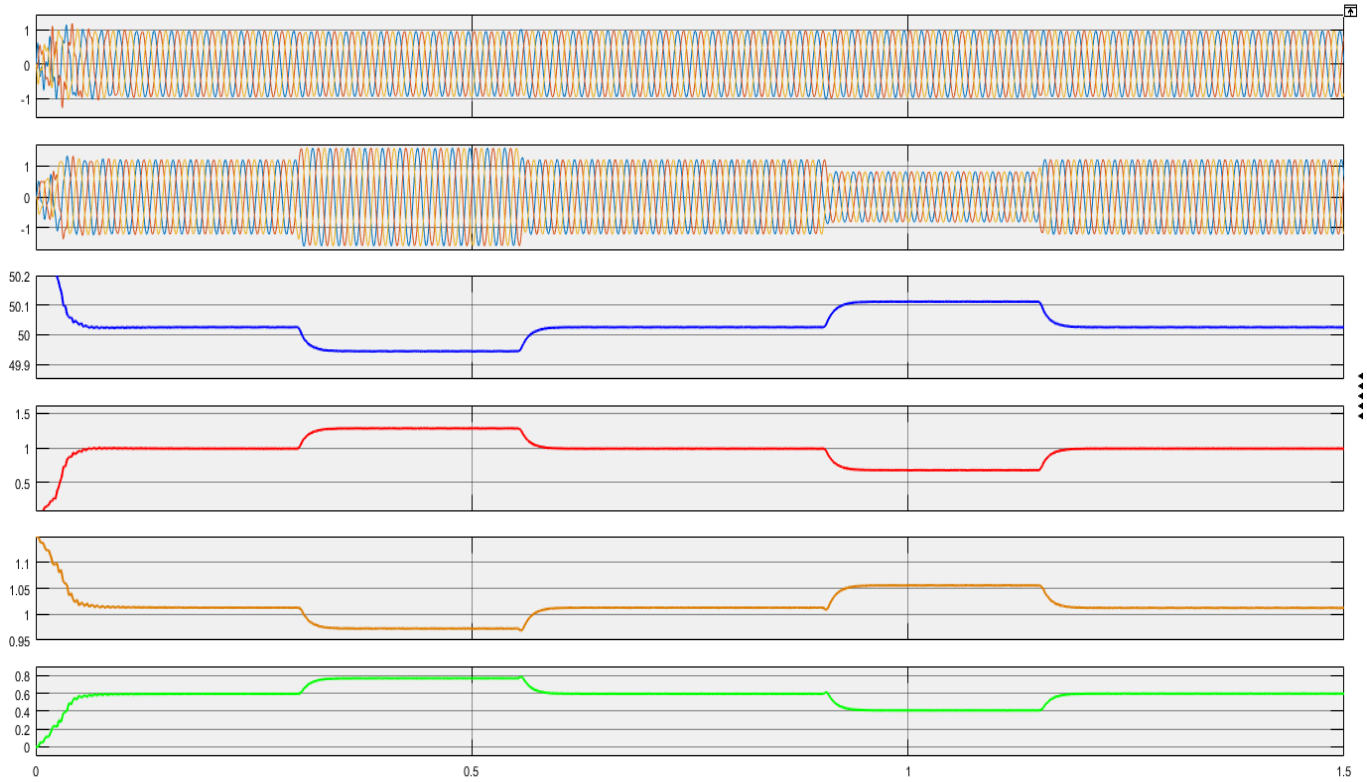


Figure 5.2.4 V, I, f, P, E and Q when an impedance load is switched on from $t = 0.3$ to 0.55 s and switched off from $t = 0.9$ to 1.15 s.

Summary of Result Analyses and Discussion

The uncontrolled system was characterized by power and frequency oscillations, necessitating the need for a controller.

The simulated control scheme achieved the following;

1. Improved power and frequency oscillations, hence, better power system stability and operation.
2. Emulated the SG in terms of active power and reactive power control and inertia.
3. Demonstrated the active power-frequency (P-f) and reactive power-voltage (Q-v) droop characteristics.

6. CONCLUSION AND FUTURE WORK

6.1 Conclusion

This research presents the performance of an islanded microgrid which supplies power to a load through an inverter; the energy source of the microgrid is a dc battery. A proposed droop control and emulation of inertia control of the inverter was implemented. This control scheme is important because RESs based DGs incorporate grid-feeding and grid-forming inverters which inherently offer unsatisfactory operation while both real and reactive loads are connected. Power and frequency oscillations and high rate of change of frequency result in such modes of operation. To mitigate these issues, the VSG idea emerged with inverter-based DGs. In VSG, an inverter is controlled in a way so that it can emulate the behaviour of a conventional synchronous generator efficiently to utilize its advantages in stabilization and controllability.

The relationship between active and reactive power flows, frequency and/or voltage magnitude was presented and formed the basis for power system control. A study of how the synchronous generator can be used to offer primary and secondary control of the active and reactive power of a grid was presented. Also, a research into a control scheme which replicates the inherent synchronization mechanism of the SG in the operation of inverters was presented. This research showed how power inverters could emulate the synchronous generator in terms of active and reactive power control, inertia and damping of oscillations.

Simulation results of the micro grid system with the proposed control scheme and an uncontrolled scheme for both real and reactive power load was presented. The response of this microgrid system to variations in real and reactive power was also presented. Thereby, demonstrating the emulation of active power-frequency (P-f) and reactive power-voltage (Q-v) droop control of a voltage source inverter.

This proposed VSG concept can be widely applied because of the large proportion of the inverter based RESs units. The disadvantage is the need for added electronics and complex control system to regulate these inverters.

6.2 Future Work

This section outlines four possible areas of extension or improvement of this research.

1. For the voltage and current control design, the PI controller gains (for current control) has been chosen by trial and error. Thus, we need to develop and analyse a mathematical model of the system,

and determine controller gains based on control theoretic concepts. This would improve the reproducibility and flexibility with regards to system voltage and loading.

2. An improvement can be made to the proposed VSG by introducing secondary control. This is where frequency deviations during disturbances (sudden change in resistive load) would be corrected with the help of an external energy storage.
3. In power systems, multiple generators are connected and do the load sharing to keep the system stable. However, grid connected operation was not included in the simulation. Experiments will have to be conducted to evaluate the controller performance in larger test systems with multiple inverter controllers. Also, for high penetration of inverter based RESs, it is necessary that the renewable generator bus acts as a PV-bus that maintains a desired voltage at the bus while supplying the required real and active power to the load. Changes would have to be implemented in the control scheme to achieve this.
4. This research evaluates the system stability assuming loads are balanced and nonlinear. However, in grid connected operation, experiments must be conducted for unbalanced and non-linear loads as well for the proper utilization of the proposed system.

7. REFERENCES

- [1] D. Jones and J. et al Huscher, ‘Europe’ s dark cloud’, p. 31, 2016, [Online]. Available: https://www.env-health.org/wp-content/uploads/2018/12/HEAL-Lignite-Briefing-en_web.pdf.
- [2] M. Larsson, *Global Energy Transformation*. 2009.
- [3] C. Globe, ‘Virtual inertia: Current trends and future directions’, *Appl. Sci.*, vol. 7, no. 7, pp. 1–29, 2017, doi: 10.3390/app7070654.
- [4] ‘What is Synchronous Generators? - Circuit Globe’. <https://circuitglobe.com/synchronous-generators.html> (accessed Aug. 08, 2021).
- [5] P. M. Dusane, M. Dang, F. O. Igbinoia, and G. Fandi, ‘Analysis of the Synchronous Machine in its Operational Modes : Motor , Generator and Compensator’, no. May, 2015.
- [6] H. Sun, ‘Adjustment of Active and Reactive Power of Synchronous Generator in Grid-connected Operation’, *IOP Conf. Ser. Earth Environ. Sci.*, vol. 440, no. 3, 2020, doi: 10.1088/1755-1315/440/3/032004.
- [7] K. M. Cheema, ‘A comprehensive review of virtual synchronous generator’, *Int. J. Electr. Power Energy Syst.*, vol. 120, no. February, p. 106006, 2020, doi: 10.1016/j.ijepes.2020.106006.
- [8] O. O. Mohammed, A. O. Otuoze, S. Salisu, O. Ibrahim, and N. A. Rufa’i, ‘Virtual synchronous generator: an overview’, *Niger. J. Technol.*, vol. 38, no. 1, p. 153, 2019, doi: 10.4314/njt.v38i1.20.
- [9] S. D’Arco, J. A. Suul, and O. B. Fosso, ‘A Virtual Synchronous Machine implementation for distributed control of power converters in SmartGrids’, *Electr. Power Syst. Res.*, vol. 122, pp. 180–197, 2015, doi: 10.1016/j.epsr.2015.01.001.
- [10] G. Penha da Silva Júnior, T. Figueiredo do Nascimento, and L. Sales Barros, ‘Comparison of Virtual Synchronous Generator Strategies for Control of Distributed Energy Sources and Power System Stability Improvement’, 2021, doi: 10.48011/sbse.v1i1.2482.
- [11] M. Saeedian, B. Pournazarian, S. S. Seyedalipour, B. Eskandari, and E. Pouresmaeil, ‘Emulating rotational inertia of synchronous machines by a new control technique in grid-interactive converters’, *Sustain.*, vol. 12, no. 13, 2020, doi: 10.3390/su12135346.
- [12] Fang, J.; Li, H.; Tang, Y.; Blaabjerg, F. Distributed Power System Virtual Inertia Implemented by Grid-Connected Power Converters. *IEEE Trans. Power Electron.* **2018**, 33, 8488–8499. [CrossRef]
- [13] P. Adhikari, S. Prajapati, I. Tamrakar, U. Tamrakar, and R. Tonkoski, ‘Parallel operation of virtual synchronous machines with frequency droop control’, *2017 7th Int. Conf. Power Syst. ICPS 2017*, pp. 116–120, 2018, doi: 10.1109/ICPES.2017.8387278.
- [14] J. Li, J. Zhou, and Y. Shan, ‘Operation area calculation and parameter analysis of virtual synchronous machine’, *IET Conf. Publ.*, vol. 2019, no. CP764, pp. 1–10, 2019, doi: 10.1049/cp.2019.0276.
- [15] M. J. Tsai, Y. J. Chang, and P. T. Cheng, ‘Verification of the power converter based virtual synchronous machine’, *19th Int. Conf. Electr. Mach. Syst. ICEMS 2016*, no. 3, 2017.
- [16] M. Lomme, ‘Modeling of a Microgrid: Power Sharing in Synchronous Generators and Inverters’, *Long Range Plann.*, vol. 9, no. 1, p. 92, 2015.

- [17] ‘Synchronization (alternating current) - Wikipedia’. [https://en.wikipedia.org/wiki/Synchronization_\(alternating_current\)](https://en.wikipedia.org/wiki/Synchronization_(alternating_current)) (accessed Sep. 24, 2021).
- [18] ‘Introduction to Synchronous Generator, Working, Construction, Types & Applications - The Engineering Knowledge’. <https://www.theengineeringknowledge.com/introduction-to-synchronous-generator/> (accessed Aug. 16, 2021).
- [19] A. Islam, ‘Implementation of Virtual Synchronous Generator Methodologies For Renewable Integration’, 2017, [Online]. Available: [https://www.oecd.org/dac/accountable-effective-institutions/Governance Notebook 2.6 Smoke.pdf](https://www.oecd.org/dac/accountable-effective-institutions/Governance%20Notebook%202.6%20Smoke.pdf).
- [20] Y. Zheng, *Virtual Inertia Emulation in island microgrids with energy storage system*. 2016.
- [21] M. A. Hossain, H. R. Pota, W. Issa, and M. J. Hossain, ‘Overview of AC microgrid controls with inverter-interfaced generations’, *Energies*, vol. 10, no. 9, pp. 1–27, 2017, doi: 10.3390/en10091300.
- [22] D. Pattabiraman, R. H. Lasseter, and T. M. Jahns, ‘Comparison of Grid Following and Grid Forming Control for a High Inverter Penetration Power System’, *IEEE Power Energy Soc. Gen. Meet.*, vol. 2018-August, pp. 1–5, 2018, doi: 10.1109/PESGM.2018.8586162.